SIAM J. SCI. COMPUT.
Vol. 45, No. 2, pp. A554–A578

$\mathcal{L}_2$-OPTIMAL REDUCED-ORDER MODELING USING PARAMETER-SEPARABLE FORMS*

PETAR MLINARIĆ† AND SERKAN GUGERCIN‡

Abstract. We provide a unifying framework for $\mathcal{L}_2$-optimal reduced-order modeling for linear time-invariant dynamical systems and stationary parametric problems. Using parameter-separable forms of the reduced-model quantities, we derive the gradients of the $\mathcal{L}_2$ cost function with respect to the reduced matrices, which then allows a nonintrusive, data-driven, gradient-based descent algorithm to construct the optimal approximant using only output samples. By choosing an appropriate measure, the framework covers both continuous (Lebesgue) and discrete cost functions. We show the efficacy of the proposed algorithm via various numerical examples. Furthermore, we analyze under what conditions the data-driven approximant can be obtained via projection.

Key words. reduced-order modeling, parametric stationary problems, linear time-invariant systems, optimization, $\mathcal{L}_2$ norm, nonlinear least squares

MSC codes. 46N10, 65K05, 93A15, 93B40

DOI. 10.1137/22M1500678

1. Introduction.

Consider a parameter-to-output mapping

$$y\colon \mathcal{P} \to \mathbb{C}^{n_\mathrm{o}\times n_\mathrm{f}}, \quad \mathsf{p} \mapsto y(\mathsf{p}), \tag{1.1}$$

where $\mathcal{P} \subseteq \mathbb{C}^{n_\mathrm{p}}$ denotes the parameter space, and $n_\mathrm{p}, n_\mathrm{f}, n_\mathrm{o}$ are positive integers, representing the parameter, forcing (input), and output dimensions of the underlying parametric model. We are interested in cases where evaluating $y(\mathsf{p})$ for a given p is expensive (thus causing a computational bottleneck in *online* computations) and we only have access to (the output) $y(\mathsf{p})$ without access to an internal representation.

Our goal is to construct a data-driven reduced-order model (DDROM)

$$\widehat{\mathcal{A}}(\mathsf{p})\widehat{x}(\mathsf{p}) = \widehat{\mathcal{B}}(\mathsf{p}), \tag{1.2a}$$

$$\widehat{y}(\mathsf{p}) = \widehat{\mathcal{C}}(\mathsf{p})\widehat{x}(\mathsf{p}), \tag{1.2b}$$

whose output $\widehat{y}(\mathsf{p})$ is significantly cheaper to evaluate compared to $y(\mathsf{p})$, and $\widehat{y}(\mathsf{p})$ is close to $y(\mathsf{p})$ for all $\mathsf{p} \in \mathcal{P}$. In (1.2) we have $\widehat{\mathcal{A}}(\mathsf{p}) \in \mathbb{C}^{r\times r}$, $\widehat{\mathcal{B}}(\mathsf{p}) \in \mathbb{C}^{r\times n_\mathrm{f}}$, $\widehat{\mathcal{C}}(\mathsf{p}) \in \mathbb{C}^{n_\mathrm{o}\times r}$, $\widehat{x}(\mathsf{p}) \in \mathbb{C}^{r\times n_\mathrm{f}}$, and $\widehat{y}(\mathsf{p}) \in \mathbb{C}^{n_\mathrm{o}\times n_\mathrm{f}}$, where r is a modest integer so that evaluating $\widehat{y}(\mathsf{p})$ via (1.2) is trivial. The modeling structure in (1.2) is motivated by model order reduction for stationary parametric partial differential equations (PDEs) and linear time-invariant (LTI) dynamical systems, as we briefly explain next.

* Submitted to the journal's Methods and Algorithms for Scientific Computing section June 7, 2022; accepted for publication (in revised form) October 20, 2022; published electronically April 26, 2023.

https://doi.org/10.1137/22M1500678

Funding: This work was partially funded by the U.S. National Science Foundation under grant DMS-1923221. Parts of this material are based upon work supported by the National Science Foundation under grant DMS-1929284 while the authors were in residence at the Institute for Computational and Experimental Research in Mathematics in Providence, RI, during the spring 2020 Reunion Event for Model and Dimension Reduction in Uncertain and Dynamic Systems program.

† Department of Mathematics, Virginia Tech, Blacksburg, VA 24061 USA (mlinaric@vt.edu).

‡ Department of Mathematics and Division of Computational Modeling and Data Analytics, Academy of Data Science, Virginia Tech, Blacksburg, VA 24061 USA (gugercin@vt.edu).

First, consider a parameterized linear PDE in the weak form

$$a(\xi(\mathsf{p}),\zeta;\mathsf{p}) = f(\zeta;\mathsf{p}) \quad \forall \zeta \in \mathcal{X}, \tag{1.3a}$$

$$q(\mathsf{p}) = l(\xi(\mathsf{p});\mathsf{p}), \tag{1.3b}$$

where $\mathsf{p} \in \mathcal{P} \subseteq \mathbb{R}^{n_\mathrm{p}}$ is the parameter, $\mathcal{X}$ is a real Hilbert space, $\xi(\mathsf{p}) \in \mathcal{X}$ is the solution, and $q(\mathsf{p}) \in \mathbb{R}$ is the quantity of interest. Furthermore, $a(\cdot,\cdot;\mathsf{p})\colon \mathcal{X}\times\mathcal{X} \to \mathbb{R}$ is a coercive and continuous bilinear form and $f(\cdot;\mathsf{p}), l(\cdot;\mathsf{p})\colon \mathcal{X} \to \mathbb{R}$ are bounded linear functionals for all $\mathsf{p} \in \mathcal{P}$. In the simple case with $n_\mathrm{p} = 1$, $a(\xi,\zeta;\mathsf{p}) = a_1(\xi,\zeta) + \mathsf{p}a_2(\xi,\zeta)$, $f(\zeta;\mathsf{p}) = f(\zeta)$, and $l(\xi;\mathsf{p}) = l(\xi)$, after a Galerkin projection onto an n-dimensional subspace $\operatorname{span}\{\xi_1,\xi_2,\dots,\xi_n\} \subset \mathcal{X}$ (e.g., constructed by a finite element discretization), we obtain a finite-dimensional model

$$(A_1 + \mathsf{p}A_2)x(\mathsf{p}) = B, \tag{1.4a}$$

$$y(\mathsf{p}) = Cx(\mathsf{p}), \tag{1.4b}$$

where $x(\mathsf{p}) \in \mathbb{R}^n$ is the projected solution, $y(\mathsf{p}) \in \mathbb{R}$ is the output approximating $q(\mathsf{p})$, and $A_1, A_2 \in \mathbb{R}^{n\times n}$ and $B, C^\mathrm{T} \in \mathbb{R}^{n\times 1}$ are given componentwise by $[A_1]_{ij} = a_1(\xi_j,\xi_i)$, $[A_2]_{ij} = a_2(\xi_j,\xi_i)$, $[B]_{i1} = f(\xi_i)$, and $[C]_{1j} = l(\xi_j)$. If, for example, $A_1 + \mathsf{p}A_2$ is invertible for every $\mathsf{p} \in \mathcal{P}$, then the parameter-to-output mapping in this case is given by $y(\mathsf{p}) = C(A_1 + \mathsf{p}A_2)^{-1}B$. This problem corresponds to $n_\mathrm{f} = n_\mathrm{o} = 1$. Note that n_f here represents the number of right-hand sides in (1.4a), i.e., the number of forcing terms. If, in addition, the problem (1.3) is compliant, i.e., $a(\cdot,\cdot;\mathsf{p})$ is symmetric and $l = f$, then A_1 and A_2 are symmetric and $C = B^\mathrm{T}$.

Now, consider an LTI dynamical system described in state space as

$$E\dot{x}(t) = Ax(t) + Bu(t), \quad x(0) = 0, \tag{1.5a}$$

$$y(t) = Cx(t), \tag{1.5b}$$

where $t \in \mathbb{R}$ is the time, $u(t) \in \mathbb{R}^{n_\mathrm{f}}$ is the input, $x(t) \in \mathbb{R}^n$ is the state, $y(t) \in \mathbb{R}^{n_\mathrm{o}}$ is the output, $E, A \in \mathbb{R}^{n\times n}$, $B \in \mathbb{R}^{n\times n_\mathrm{f}}$, and $C \in \mathbb{R}^{n_\mathrm{o}\times n}$. By applying the Laplace transform to (1.5), we obtain $Y(s) = H(s)U(s)$, where U and Y are, respectively, the Laplace transforms of u and y. Furthermore, $H(s) \in \mathbb{C}^{n_\mathrm{o}\times n_\mathrm{f}}$ is given by

$$H(s) = C(sE - A)^{-1}B \tag{1.6}$$

and is called the transfer function, which is at the heart of systems-theoretic approaches to optimal approximation of LTI systems [3, 1]. We can rewrite $H(s)$ as

$$(sE - A)X(s) = B, \tag{1.7a}$$

$$H(s) = CX(s) \tag{1.7b}$$

for any $s \in \mathbb{C}$ such that $sE - A$ is invertible and $X(s) \in \mathbb{C}^{n\times n_\mathrm{f}}$.

Therefore, both mappings, namely $\mathsf{p} \mapsto q(\mathsf{p})$ in (1.3) and $s \mapsto H(s)$ in (1.6), are examples of parameter-to-output mappings (1.1) we consider in this paper. Both models (1.4) (resulting from discretization of a stationary parametric PDE) and (1.7) (frequency domain formulation of an LTI system) can be examined using the form

$$\mathcal{A}(\mathsf{p})x(\mathsf{p}) = \mathcal{B}(\mathsf{p}), \tag{1.8a}$$

$$(\mathsf{p}) = \mathcal{C}(\mathsf{p})x(\mathsf{p}), \tag{1.8b}$$

where $\mathsf{p} \in \mathcal{P} \subseteq \mathbb{C}^{n_\mathrm{p}}$ is the parameter, $x(\mathsf{p}) \in \mathbb{C}^{n \times n_\mathrm{f}}$ is the state, $y(\mathsf{p}) \in \mathbb{C}^{n_\mathrm{o} \times n_\mathrm{f}}$ is the output, $\mathcal{A}(\mathsf{p}) \in \mathbb{C}^{n \times n}$, $\mathcal{B}(\mathsf{p}) \in \mathbb{C}^{n \times n_\mathrm{f}}$, and $\mathcal{C}(\mathsf{p}) \in \mathbb{C}^{n_\mathrm{o} \times n}$. Many applications require solving the model (1.8) in real time or for many parameter values, which incurs a computational bottleneck due to the large-scale dimension of the underlying state-space. The goal of model order reduction for parametric PDEs and for LTI systems is to replace (1.8) with a reduced-order model (ROM), which motivates us to approximate the mapping (1.1) by the DDROM of the form (1.2).

Thus the framework we consider handles a wide range of problems (stationary or dynamic), including those of the form in (1.8). We revisit both problems (1.4) and (1.7) throughout the paper and illustrate how the theory applies in either case. Furthermore, even though the motivation comes from full-order models (FOMs) of the form in (1.8), the approximation framework we develop below only requires access to the parameter-to-output mapping (1.1) and *not* to the full-order operators $\mathcal{A}$, $\mathcal{B}$, $\mathcal{C}$ and state x. Thus, we work with a nonintrusive parameter/output data-driven formulation. Therefore, we refer to our methodology as "reduced-order modeling" instead of "model order reduction."

It is worth mentioning that a similar setting of a parameter-to-output mapping appears in, e.g., active subspaces [13]. As [13] focuses on parameter reduction, we believe it could be used in combination with the approach we propose here to develop a combined parameter and state reduction method (such as in [24]).

There are different ways of measuring the distance between y and $\widehat{y}$. For instance, reduced basis (RB) methods [7] are based on the $\mathcal{L}_\infty$ norm

$$\|y - \widehat{y}\|_{\mathcal{L}_\infty} = \sup_{\mathsf{p} \in \mathcal{P}} \|y(\mathsf{p}) - \widehat{y}(\mathsf{p})\|_\mathrm{F},$$

where $\|\cdot\|_\mathrm{F}$ is the Frobenius norm. For LTI systems, the corresponding measure is the $\mathcal{H}_\infty$ norm and we refer the reader to recent optimization-based algorithms for (structure-preserving) $\mathcal{H}_\infty$-optimal model order reduction [29, 40].

In this paper, we focus on a different norm. Motivated by the work on $\mathcal{H}_2$-optimal model order reduction [19, 18, 2] for nonparametric LTI systems, and extensions to $\mathcal{H}_2 \otimes \mathcal{L}_2$-optimal model order reduction [5, 36, 17, 26] for parametric LTI systems, we are interested in $\mathcal{L}_2$-optimal reduced-order modeling for parametric problems (1.1). Specifically, we are interested in finding a DDROM (1.2) that minimizes the $\mathcal{L}_2$ error

$$\|y - \widehat{y}\|_{\mathcal{L}_2} = \left(\int_{\mathcal{P}} \|y(\mathsf{p}) - \widehat{y}(\mathsf{p})\|_\mathrm{F}^2 \, \mathrm{d}\mathsf{p} \right)^{1/2}.$$

The goal is to develop the analysis (and the resulting computational tools) so that the framework equally applies to parametric stationary problems as in (1.4) and to dynamical systems as in (1.5) by the proper definition of the parameter space and error measure. Additionally, we want the analysis to be applicable to more general measures μ over the parameter space $\mathcal{P}$, i.e., minimizing

$$\|y - \widehat{y}\|_{\mathcal{L}_2(\mathcal{P},\mu)} = \left(\int_{\mathcal{P}} \|y(\mathsf{p}) - \widehat{y}(\mathsf{p})\|_\mathrm{F}^2 \, \mathrm{d}\mu(\mathsf{p}) \right)^{1/2}. \tag{1.9}$$

For example, μ could be a probability measure over $\mathcal{P}$ and the parameter p could be treated as a random variable. Another example of a measure is a discrete measure

$\mu_{\mathrm{d}} = \sum_{i=1}^{N} \delta_{\mathsf{p}_i}$, where δ_x is the Dirac measure ($\delta_x(A) = |\{x\} \cap A|$) and $\mathsf{p}_1, \mathsf{p}_2, \ldots, \mathsf{p}_N$ are some parameter values, which results in the error measure

$$\|y - \widehat{y}\|_{\mathcal{L}_2(\mathcal{P},\mu_{\mathrm{d}})} = \left(\sum_{i=1}^{N} \|y(\mathsf{p}_i) - \widehat{y}(\mathsf{p}_i)\|_{\mathrm{F}}^2 \right)^{1/2}.$$

Therefore, we develop theoretical results that hold for both continuous and discrete objective functions.

We note that the objective (1.9) is reminiscent of operator inference [35]. However, the fundamental difference is that operator inference solves a linear least-squares problem, while we solve a nonlinear optimization problem. This is due to the fact that while operator inference minimizes the residual, our goal is to minimize the output error. Furthermore, operator inference requires, in its original formulation, full state snapshots, while our approach only needs output measurements. Additionally, operator inference is usually posed in the time domain, unlike our $\mathcal{L}_2$ measure, which would be posed in the Laplace/frequency domain.

The main contributions of the paper are as follows:

- We develop a unifying formulation for $\mathcal{L}_2$-optimal data-driven reduced-order modeling, which applies to a wide range of problems with an appropriate definition of the measure space.
- We derive explicit formulae for gradients of the $\mathcal{L}_2$ approximation error with respect to the matrices of the DDROM. These gradient computations require access only to the model output without internal (state) samples.
- Based on the gradient formulae, we develop a data-driven, gradient-based algorithm for $\mathcal{L}_2$-optimal reduced-order modeling.
- We extend the framework to a discrete least-squares error function.
- We analyze and give conditions under which the $\mathcal{L}_2$-optimal DDROM can be obtained via projection.

The rest of the paper is organized as follows. In subsection 1.1 we briefly recall projection-based model order reduction, the most common framework for intrusive model order reduction. We state the structured $\mathcal{L}_2$-optimal reduced-order modeling problem in section 2 and derive the gradients of the squared $\mathcal{L}_2$ error with respect to the matrices of the DDROM. Furthermore, there we discuss a generic optimization-based algorithm for $\mathcal{L}_2$-optimal reduced-order modeling. In section 3 we focus on the continuous objective function and provide numerical examples. Then, we discuss discrete objective function in section 4, where we demonstrate the generic algorithm on further examples. In section 5 we return to projection-based model order reduction and discuss whether $\mathcal{L}_2$-optimal DDROMs are projection-based. Finally, section 6 gives concluding remarks.

1.1. Projection-based model order reduction. Even though our framework is data-driven and does not start with or need a FOM to reduce, in this section, we briefly recall the basics of the projection-based model order reduction methods to help motivate the structure enforced on the DDROM (1.2).

For a FOM (1.8), the Petrov–Galerkin projection framework is one of the most common ways to construct the ROM (1.2). In this framework, given the FOM (1.8), one chooses two r-dimensional subspaces of $\mathbb{R}^n$, spanned by the columns of $V, W \in \mathbb{R}^{n \times r}$, and constructs the ROM (1.2) by

$$\widehat{\mathcal{A}}(\mathsf{p}) = W^{\mathrm{T}} \mathcal{A}(\mathsf{p}) V, \quad \widehat{\mathcal{B}}(\mathsf{p}) = W^{\mathrm{T}} \mathcal{B}(\mathsf{p}), \quad \widehat{\mathcal{C}}(\mathsf{p}) = \mathcal{C}(\mathsf{p}) V. \tag{1.10}$$

If V and W span the same subspace, this is called a Galerkin projection.

Even though $\widehat{\mathcal{A}}(\mathsf{p}) \in \mathbb{C}^{r\times r}$, $\widehat{\mathcal{B}}(\mathsf{p}) \in \mathbb{C}^{r\times n_{\mathrm{f}}}$, $\widehat{\mathcal{C}}(\mathsf{p}) \in \mathbb{C}^{n_{\mathrm{o}}\times r}$ in (1.10) have the reduced row and/or column dimensions, evaluating them for a new parameter value p requires operations in the full dimension n. Thus, for efficient computation of the ROM, it is often assumed that the FOM matrices have a parameter-separable form (or that it can be approximated by one, e.g., using the empirical interpolation method [4]), i.e.,

$$\mathcal{A}(\mathsf{p}) = \sum_{i=1}^{q_{\mathcal{A}}} \alpha_i(\mathsf{p}) A_i, \quad \mathcal{B}(\mathsf{p}) = \sum_{j=1}^{q_{\mathcal{B}}} \beta_j(\mathsf{p}) B_j, \quad \mathcal{C}(\mathsf{p}) = \sum_{k=1}^{q_{\mathcal{C}}} \gamma_k(\mathsf{p}) C_k, \tag{1.11}$$

where $q_{\mathcal{A}}, q_{\mathcal{B}}, q_{\mathcal{C}}$ are small positive integers, $\alpha_i, \beta_j, \gamma_k \colon \mathcal{P} \to \mathbb{C}$ are given functions that are easy to evaluate, and $A_i \in \mathbb{R}^{n\times n}$, $B_j \in \mathbb{R}^{n\times n_{\mathrm{f}}}$, $C_k \in \mathbb{R}^{n_{\mathrm{o}}\times n}$ are constant matrices. Then, one computes the ROM matrices

$$\widehat{A}_i = W^{\mathrm{T}} A_i V, \quad \widehat{B}_j = W^{\mathrm{T}} B_j, \quad \widehat{C}_k = C_k V \tag{1.12}$$

only once, and the ROM (1.2) is constructed efficiently as

$$\widehat{\mathcal{A}}(\mathsf{p}) = \sum_{i=1}^{q_{\mathcal{A}}} \alpha_i(\mathsf{p}) \widehat{A}_i, \quad \widehat{\mathcal{B}}(\mathsf{p}) = \sum_{j=1}^{q_{\mathcal{B}}} \beta_j(\mathsf{p}) \widehat{B}_j, \quad \widehat{\mathcal{C}}(\mathsf{p}) = \sum_{k=1}^{q_{\mathcal{C}}} \gamma_k(\mathsf{p}) \widehat{C}_k. \tag{1.13}$$

Thus, the full-order operators $\mathcal{A}(\mathsf{p}), \mathcal{B}(\mathsf{p}), \mathcal{C}(\mathsf{p})$ are avoided when solving the ROM. There are many projection-based model order reduction methods and thus many different ways of computing V and W; see, e.g., [8, 7, 1, 3, 9, 38, 23, 10]. We revisit some of these methods in more detail in section 3.

2. $\mathcal{L}_2$-optimal reduced-order modeling.

In this section, we first establish the setting of the optimal reduced-order modeling problem we consider and prove the main theoretical result that forms the foundation of the proposed algorithm.

2.1. Setting.

We are interested in approximating a parameter-to-output mapping (1.1) by a DDROM (1.2). Although the motivation comes from the form of FOMs as in (1.8), the framework we develop here does not require the full-order operators $\mathcal{A}$, $\mathcal{B}$, and $\mathcal{C}$ or the full-order state x. Instead we only need (the samples of) the output y. In other words, we develop an optimal data-driven approximation formulation that only uses the parameter/output samples of the model under consideration. More specifically, we consider the FOMs accessible only via a complex-valued output function $y \colon \mathcal{P} \to \mathbb{C}^{n_{\mathrm{o}}\times n_{\mathrm{f}}}$, where $\mathcal{P} \subseteq \mathbb{C}^{n_{\mathrm{p}}}$ and $(\mathcal{P}, \Sigma, \mu)$ is a measure space.

We make some technical assumptions on the FOM valid for the general setup we consider here. Then by revisiting the specific FOMs in (1.4) and (1.7), we show that these are common assumptions and they automatically hold in most cases.

Assumption 2.1 (FOM assumptions). Let $(\mathcal{P}, \Sigma, \mu)$ be a measure space and $y \colon \mathcal{P} \to \mathbb{C}^{n_{\mathrm{o}}\times n_{\mathrm{f}}}$ a measurable function.

- The set $\mathcal{P} \subseteq \mathbb{C}^{n_{\mathrm{p}}}$ is closed under conjugation ($\overline{\mathsf{p}} \in \mathcal{P}$ for all $\mathsf{p} \in \mathcal{P}$).
- The σ-algebra Σ is closed under conjugation ($\overline{S} \in \Sigma$ for all $S \in \Sigma$).
- The measure μ is closed under conjugation ($\mu(\overline{S}) = \mu(S)$ for all $S \in \Sigma$).
- The function y is square-integrable ($\|y\|_{\mathcal{L}_2(\mathcal{P},\mu)} < \infty$) and closed under conjugation ($\overline{y(\mathsf{p})} = y(\overline{\mathsf{p}})$ for all $\mathsf{p} \in \mathcal{P}$).

Example 2.2. We revisit the two basic examples from section 1 under the setting of Assumption 2.1. First consider the FOM (1.4) resulting from the discretization of a stationary parametric PDE. Let $\mathcal{P} = [a, b] \subset \mathbb{R}$ and μ be the Lebesgue measure. Then, Assumption 2.1 holds if $A_1 + \mathsf{p}A_2$ is invertible for all $\mathsf{p} \in \mathcal{P}$, a common assumption.

Now, recall the transfer function (1.6) of an LTI system (1.5) formulated as a parametric stationary problem (1.7). One commonly used system norm is the Hardy $\mathcal{H}_2$ norm $\|\cdot\|_{\mathcal{H}_2}$, which gives the output bound $\|y\|_{\mathcal{L}_\infty} \leqslant H\|u\|_{\mathcal{L}_2}$. The norm can be formulated as $\|H\|_{\mathcal{H}_2} = (\frac{1}{2\pi}\int_{-\infty}^{\infty} \|H(\imath\omega)\|_{\mathrm{F}}^2 \mathrm{d}\omega)^{1/2}$, assuming that E is invertible and all the eigenvalues of $E^{-1}A$ have negative real parts, where $\imath$ denotes the imaginary unit. Therefore, to have $\|H\|_{\mathcal{H}_2} = \|H\|_{\mathcal{L}_2(\mathcal{P},\mu)}$, we can take $\mathsf{p} = s$, $\mathcal{P} = \imath\mathbb{R}$, and $\mu = \frac{1}{2\pi}\lambda_{\imath\mathbb{R}}$, where $\lambda_{\imath\mathbb{R}}$ is the Lebesgue measure over $\imath\mathbb{R}$. A sufficient condition for Assumption 2.1 to hold is that E be invertible and $E^{-1}A$ have no eigenvalues on the imaginary axis, which are weaker assumptions than those needed to define the $\mathcal{H}_2$ norm. These are also common assumptions in the systems-theoretic setting. One can indeed allow E to be singular (i.e., allow systems of differential algebraic equations) as has been done in many earlier works [27, 20]. However, to keep the notation and discussion concise, we assume E to be invertible.

2.2. Optimization problem with parameter-separable forms. Given the parameter-to-output mapping in (1.1), our goal is to find a DDROM (1.2) that minimizes the output $\mathcal{L}_2$ error (1.9). As discussed in subsection 1.1, many FOMs have a parameter-separable form as in (1.11) and this form is preserved in the classical Petrov–Galerkin projection-based ROMs. Inspired by this formulation, in our $\mathcal{L}_2$-optimal DDROM setting, we search for a structured DDROM with parameter-separable form

$$\widehat{\mathcal{A}}(\mathsf{p}) = \sum_{i=1}^{q_{\widehat{\mathcal{A}}}} \widehat{\alpha}_i(\mathsf{p})\widehat{A}_i, \quad \widehat{\mathcal{B}}(\mathsf{p}) = \sum_{j=1}^{q_{\widehat{\mathcal{B}}}} \widehat{\beta}_j(\mathsf{p})\widehat{B}_j, \quad \widehat{\mathcal{C}}(\mathsf{p}) = \sum_{k=1}^{q_{\widehat{\mathcal{C}}}} \widehat{\gamma}_k(\mathsf{p})\widehat{C}_k, \tag{2.1}$$

where $q_{\widehat{\mathcal{A}}}, q_{\widehat{\mathcal{B}}}, q_{\widehat{\mathcal{C}}}$ are positive integers, $\widehat{\alpha}_i, \widehat{\beta}_j, \widehat{\gamma}_k \colon \mathcal{P} \to \mathbb{C}$ are given measurable functions, and $\widehat{A}_i \in \mathbb{R}^{r\times r}$, $\widehat{B}_j \in \mathbb{R}^{r\times n_{\mathrm{f}}}$, $\widehat{C}_k \in \mathbb{R}^{n_{\mathrm{o}}\times r}$ are the (DDROM) matrices we want to compute to minimize the $\mathcal{L}_2$ error (1.9). Note that even though the DDROM structure is inspired by the parameter-separable structures appearing in many FOMs and preserved in projection-based ROMs, here we make no assumptions on the form of the FOM, but only on the form of the DDROM. The subtle notational difference between (1.13) and (2.1), namely the "hatted" scalar functions, aims to highlight that unlike in the projection-based ROM (1.13), where the scalar functions match those of the FOM, in the DDROM (2.1), we have freedom in choosing them. We also note that this parameter-separable structure appears in [6, 26] as well.

We make the following assumptions on the scalar functions $\widehat{\alpha}_i, \widehat{\beta}_j, \widehat{\gamma}_k$ appearing in the DDROM (2.1). As we did for Assumption 2.1, later we discuss that these assumptions indeed hold trivially in many cases.

Assumption 2.3 (scalar functions). Let $\mathcal{P}$ and μ satisfy Assumption 2.1. The functions $\widehat{\alpha}_i, \widehat{\beta}_j, \widehat{\gamma}_k \colon \mathcal{P} \to \mathbb{C}$ are measurable, are closed under conjugation, and satisfy

$$\int_{\mathcal{P}} \left(\frac{\sum_{j=1}^{q_{\widehat{\mathcal{B}}}} \left|\widehat{\beta}_j(\mathsf{p})\right| \sum_{k=1}^{q_{\widehat{\mathcal{C}}}} |\widehat{\gamma}_k(\mathsf{p})|}{\sum_{i=1}^{q_{\widehat{\mathcal{A}}}} |\widehat{\alpha}_i(\mathsf{p})|} \right)^2 \mathrm{d}\mu(\mathsf{p}) < \infty. \tag{2.2}$$

Now based on Assumptions 2.1 and 2.3, we introduce the set of allowable DDROM matrices.

DEFINITION 2.4. *Let $\mathcal{P}$ and μ satisfy Assumption* 2.1 *and $\widehat{\alpha}_i, \widehat{\beta}_j, \widehat{\gamma}_k \colon \mathcal{P} \to \mathbb{C}$ satisfy Assumption* 2.3. *Next, let $R = (\mathbb{R}^{r\times r})^{q_{\widehat{\mathcal{A}}}} \times (\mathbb{R}^{r\times n_{\mathrm{i}}})^{q_{\widehat{\mathcal{B}}}} \times (\mathbb{R}^{n_{\mathrm{o}}\times r})^{q_{\widehat{\mathcal{C}}}}$ be the set of all tuples of DDROM matrices $(\widehat{A}_1, \ldots, \widehat{A}_{q_{\widehat{\mathcal{A}}}}, \widehat{B}_1, \ldots, \widehat{B}_{q_{\widehat{\mathcal{B}}}}, \widehat{C}_1, \ldots, \widehat{C}_{q_{\widehat{\mathcal{C}}}}) =: (\widehat{A}_i, \widehat{B}_j, \widehat{C}_k)$. Then, we define the set $\mathcal{R}$ of allowable DDROM matrices as*

$$\mathcal{R} = \left\{ \left(\widehat{A}_i, \widehat{B}_j, \widehat{C}_k\right) \in R : \operatorname*{ess\,sup}_{\mathsf{p}\in\mathcal{P}} \left\| \widehat{\alpha}_i(\mathsf{p}) \widehat{\mathcal{A}}(\mathsf{p})^{-1} \right\|_{\mathrm{F}} < \infty,\ i = 1, 2, \ldots, q_{\widehat{\mathcal{A}}} \right\}, \tag{2.3}$$

where $\widehat{\mathcal{A}}$ is as in (2.1).

Example 2.5. We want to illustrate that the conditions in (2.2) and (2.3) do indeed hold trivially in many cases and thus are not restrictive. Continuing with Example 2.2, we want to cover the analogous DDROMs. Starting with the parametric stationary problem, we consider

$$\begin{aligned} \left(\widehat{A}_1 + \mathsf{p}\widehat{A}_2\right) \widehat{x}(\mathsf{p}) &= \widehat{B}, \\ \widehat{y}(\mathsf{p}) &= \widehat{C}\widehat{x}(\mathsf{p}). \end{aligned}$$

For this case, we have

$$q_{\widehat{\mathcal{A}}} = 2,\ \widehat{\alpha}_1(\mathsf{p}) = 1,\ \widehat{\alpha}_2(\mathsf{p}) = \mathsf{p}; \quad q_{\widehat{\mathcal{B}}} = 1,\ \widehat{\beta}_1(\mathsf{p}) = 1; \text{ and } \quad q_{\widehat{\mathcal{C}}} = 1,\ \widehat{\gamma}_1(\mathsf{p}) = 1.$$

Therefore, the condition (2.2) becomes $\int_a^b \frac{1}{(1+|\mathsf{p}|)^2} \mathrm{d}\mathsf{p} < \infty$, which holds true. The condition in (2.3) states that $\mathsf{p} \mapsto \widehat{\mathcal{A}}(\mathsf{p})^{-1}$ and $\mathsf{p} \mapsto \mathsf{p}\widehat{\mathcal{A}}(\mathsf{p})^{-1}$ are bounded over $[a, b]$. The necessary and sufficient condition is that $\widehat{\mathcal{A}}(\mathsf{p})$ be invertible for all $\mathsf{p} \in \mathcal{P}$.

Next, we consider a reduced-order LTI system

$$\left(s\widehat{E} - \widehat{A}\right) \widehat{X}(s) = \widehat{B}, \tag{2.4a}$$

$$\widehat{H}(s) = \widehat{C}\widehat{X}(s). \tag{2.4b}$$

For this case, we have

$$q_{\widehat{\mathcal{A}}} = 2,\ \widehat{\alpha}_1(\mathsf{p}) = \mathsf{p},\ \widehat{\alpha}_2(\mathsf{p}) = -1; \quad q_{\widehat{\mathcal{B}}} = 1,\ \widehat{\beta}_1(\mathsf{p}) = 1; \text{ and } \quad q_{\widehat{\mathcal{C}}} = 1,\ \widehat{\gamma}_1(\mathsf{p}) = 1,$$

with $\mathsf{p} = s = \imath\omega$. The condition (2.2) becomes $\int_{-\infty}^{\infty} \frac{1}{(|\omega|+1)^2} \mathrm{d}\omega < \infty$, which also holds. Finally, the condition in (2.3) states that $s \mapsto (s\widehat{E} - \widehat{A})^{-1}$ and $s \mapsto s(s\widehat{E} - \widehat{A})^{-1} = (\widehat{E} - \frac{1}{s}\widehat{A})^{-1}$ are bounded over $\imath\mathbb{R}$. This is equivalent to the invertibility of $\widehat{E}$ and $\widehat{E}^{-1}\widehat{A}$ having no eigenvalues in $\imath\mathbb{R}$, similar to the FOM discussed in Example 2.2.

The choice of functions $\widehat{\alpha}_i, \widehat{\beta}_j, \widehat{\gamma}_k \colon \mathcal{P} \to \mathbb{C}$ is flexible as long as they satisfy Assumption 2.3. In many cases, such as for LTI systems as above, physically inspired choices are immediately available from the underlying physics.

For the analysis in subsection 2.3, it is important to establish that the set $\mathcal{R}$ (2.3) is open and that it forms a set of feasible DDROMs. This is what we do next.

LEMMA 2.6. *The set $\mathcal{R}$* (2.3) *in Definition* 2.4 *is open. Moreover, for all $\widehat{y}$ defined by a DDROM $(\widehat{A}_i, \widehat{B}_j, \widehat{C}_k) \in \mathcal{R}$, we have that $\widehat{y}$ is square-integrable.*

Proof. The proof of this result is given in Appendix A. ∎

2.3. Computing the gradients. In this section, we derive one of the main results of this paper, mainly the gradients of the $\mathcal{L}_2$ cost function (1.9) with respect

to the DDROM matrices $\widehat{A}_i, \widehat{B}_j, \widehat{C}_k$. These gradient formulae form the foundation of the $\mathcal{L}_2$-optimal reduced-order modeling algorithm we develop.

Given the FOM as a parameter-to-output mapping y (1.1), we want to construct a DDROM (1.2) with the structured reduced-order matrices of the form (2.1). Furthermore, we look for a DDROM belonging to $\mathcal{R}$ from Definition 2.4, since this guarantees that the squared $\mathcal{L}_2$ error is well-defined and differentiable over $\mathcal{R}$ (as shown in Theorem 2.7) without substantial restrictions on the form of the DDROM. Thus, we consider the structured $\mathcal{L}_2$-optimization problem

$$\underset{(\widehat{A}_i,\widehat{B}_j,\widehat{C}_k)\in\mathcal{R}}{\text{minimize}} \quad \mathcal{J}\left(\widehat{A}_i,\widehat{B}_j,\widehat{C}_k\right) = \|y-\widehat{y}\|^2_{\mathcal{L}_2(\mathcal{P},\mu)}.$$

In our analysis below, we also employ the reduced-order *dual state* $\widehat{x}_d(\mathsf{p})$, satisfying the reduced-order dual state equation $\widehat{\mathcal{A}}(\mathsf{p})^*\widehat{x}_d(\mathsf{p}) = \widehat{\mathcal{C}}(\mathsf{p})^*$ [16], where $(\cdot)^*$ denotes the conjugate transpose of a matrix.

Before establishing the gradients of the objective function $\mathcal{J}$ with respect to the DDROM matrices, we recall some notation. For a Fréchet differentiable function $f\colon U \to \mathbb{R}$, defined on an open subset U of a Hilbert space H with inner product $\langle\cdot,\cdot\rangle$, the gradient of f at x, denoted $\nabla f(x)$, is the unique element of H satisfying $f(x+h) = f(x) + \langle \nabla f(x),\, h\rangle + o(\|h\|)$, where $g(h) = o(\|h\|)$ denotes that $\lim_{h\to 0} g(h)/\|h\| = 0$. For a multivariate function $f(x_1, x_2, \ldots, x_k)$, partial gradients $\nabla_{x_i} f(x_1, x_2, \ldots, x_k)$ are defined in a similar way.

THEOREM 2.7. *Let $\mathcal{P}$, μ, and y satisfy Assumption* 2.1 *and $(\widehat{A}_i, \widehat{B}_j, \widehat{C}_k)$ be a tuple of DDROM matrices belonging to $\mathcal{R}$* (2.3). *Then, the gradients of $\mathcal{J}$ with respect to the DDROM matrices are*

$$\nabla_{\widehat{A}_i}\mathcal{J} = 2\int_{\mathcal{P}} \widehat{\alpha}_i(\overline{\mathsf{p}})\widehat{x}_d(\mathsf{p})\left[y(\mathsf{p}) - \widehat{y}(\mathsf{p})\right]\widehat{x}(\mathsf{p})^*\mathrm{d}\mu(\mathsf{p}), \qquad i = 1,2,\ldots,q_{\widehat{\mathcal{A}}},$$

$$\nabla_{\widehat{B}_j}\mathcal{J} = 2\int_{\mathcal{P}} \widehat{\beta}_j(\overline{\mathsf{p}})\widehat{x}_d(\mathsf{p})\left[\widehat{y}(\mathsf{p}) - y(\mathsf{p})\right]\mathrm{d}\mu(\mathsf{p}), \qquad j = 1,2,\ldots,q_{\widehat{\mathcal{B}}},$$

$$\nabla_{\widehat{C}_k}\mathcal{J} = 2\int_{\mathcal{P}} \widehat{\gamma}_k(\overline{\mathsf{p}})\left[\widehat{y}(\mathsf{p}) - y(\mathsf{p})\right]\widehat{x}(\mathsf{p})^*\mathrm{d}\mu(\mathsf{p}), \qquad k = 1,2,\ldots,q_{\widehat{\mathcal{C}}}.$$

Proof. The expressions follow from using the definition of the gradient, Assumptions 2.1 and 2.3, Definition 2.4, and the result of Lemma 2.6 to show differentiability. The full proof is given in Appendix B. ∎

Note that these gradient computations do not require access to the full-order matrices or the full-order state. They are computed directly from the evaluations of the output $y(\mathsf{p})$ of the FOM. This allows us to develop a nonintrusive, data-driven, optimization-based, reduced-order modeling algorithm that only needs access to the output $y(\mathsf{p})$ of the FOM. With data-driven access to these gradient evaluations, we can design a variety of optimization algorithms to construct an $\mathcal{L}_2$-optimal DDROM for different scenarios. We discuss these details in the next subsection.

Remark 2.8. The $\mathcal{L}_2$ norm in (1.9) recovers both the $\mathcal{H}_2$ norm for nonparametric LTI systems (see Example 2.2) and the $\mathcal{H}_2 \otimes \mathcal{L}_2$ norm for parametric LTI systems by the appropriate choice of the parameter space $\mathcal{P}$ and measure μ. In particular, Theorem 2.7 has implications for interpolatory optimal reduced-order modeling of dynamical systems [3, 18, 26] and unifies optimal interpolation conditions for $\mathcal{H}_2$-optimal and $\mathcal{H}_2 \otimes \mathcal{L}_2$-optimal model order reduction of (parametric) LTI systems. These details together with interpolatory optimality conditions for approximating parametric stationary problems as in (1.4) can be found in [31].

Algorithm 2.1 $\mathcal{L}_2$-Opt-PSF.

Input: Parameter-to-output mapping y, initial guess for DDROM $(\widehat{A}_i, \widehat{B}_j, \widehat{C}_k)$, maximum number of iterations `maxit`, tolerance $\texttt{tol} > 0$.
Output: DDROM $(\widehat{A}_i, \widehat{B}_j, \widehat{C}_k)$.
1: Set $\widehat{y}^{(0)}$ as the output of the initial DDROM.
2: **for** i in $1, 2, \ldots,$ `maxit` **do**
3: Compute a new DDROM with output $\widehat{y}^{(i)}$ using a step of a gradient-based optimization method, with the squared $\mathcal{L}_2$ error (1.9) as the objective function and gradients based on Theorem 2.7.
4: **if** $\|\widehat{y}^{(i-1)} - \widehat{y}^{(i)}\|\mathcal{L}_2(\mathcal{P}, \mu)/\|\widehat{y}^{(i)}\|\mathcal{L}_2(\mathcal{P}, \mu) \leq \texttt{tol}$ **then**
5: Exit the **for** loop.
6: Return the last computed DDROM.

2.4. Algorithmic details. In this section, we describe our proposed algorithm for $\mathcal{L}_2$-optimal reduced-order modeling using parameter-separable form ($\mathcal{L}_2$-Opt-PSF). The pseudocode is given in Algorithm 2.1. As discussed earlier, from the FOM, we only need output evaluations or samples, i.e., only $y(\mathsf{p})$ is needed. $\mathcal{L}_2$-Opt-PSF does not require access to the internal state variables or full-order operators.

Some comments on the pseudocode are in order. First, the choice of the initial guess has an impact on the final result, as with any other nonconvex optimization problem. Second, we do not specify the gradient-based optimization method used in step 3. Third, the computations of the objective function and its gradient are not explicitly specified since they depend on the problem at hand. We discuss these issues in more detail in section 3. Next, in line 4, we use the relative change in the $\mathcal{L}_2$ output error as the stopping criterion, as it only depends on the reduced quantities. However, one can easily incorporate more sophisticated stopping criteria if desired. Finally, the pseudocode does not check for the invertibility of $\widehat{\mathcal{A}}(\mathsf{p})$. In our experiments, the obtained DDROMs are well-conditioned, which could be explained by the objective function increasing when $\|\widehat{\mathcal{A}}(\mathsf{p})^{-1}\|_{\mathrm{F}}$ is large.

The computational complexity of the Algorithm 2.1 depends on the size of the DDROM, more specifically on the number of unknowns, which is $q_{\widehat{\mathcal{A}}} r^2 + q_{\widehat{\mathcal{B}}} r n_{\mathrm{f}} + q_{\widehat{\mathcal{C}}} n_{\mathrm{o}} r$. Note that this is linear in the number of terms in the parameter-separable forms, the number of forcings, and the number of outputs, but quadratic in the reduced order.

3. Numerical examples for the continuous $\mathcal{L}_2$ norm. Here we present numerical experiments demonstrating the performance of $\mathcal{L}_2$-Opt-PSF (Algorithm 2.1) when μ is the Lebesgue measure (thus, a continuous least-squares problem).

In particular, we focus on the case of a one-dimensional parameter, i.e., $n_{\mathrm{p}} = 1$, where we use `quad` and `quad_vec` from `scipy.integrate` (from SciPy [41]), methods for numerical integration of scalar and vector-valued functions, respectively, to evaluate $\mathcal{J}$ (1.9) and its gradients (see Theorem 2.7). For the gradient-based optimization method in Algorithm 2.1, we chose the Broyden–Fletcher–Goldfarb–Shanno (BFGS) [33] algorithm. In Algorithm 2.1 we set $\texttt{maxit} = 1000$ and $\texttt{tol} = 10^{-6}$ for all examples. For evaluating $\mathcal{L}_\infty$ errors, we use `scipy.optimize.shgo` (from SciPy [41]), a method for global minimization.

We compare RB, proper orthogonal decomposition (POD), and $\mathcal{L}_2$-Opt-PSF. Given a training set $\mathcal{P}_{\mathrm{train}} \subseteq \mathcal{P}$ and a FOM, RB constructs the ROM via Galerkin projection, where the projection basis is built in a greedy manner to reduce the $\mathcal{L}_\infty$ error. In particular, we chose to use the strong greedy version given in Algorithm

Algorithm 3.1 Strong greedy algorithm.

Input: FOM $(\mathcal{A},\mathcal{B},\mathcal{C})$ (1.8) in parameter-separable form (1.11), finite training set $\mathcal{P}_{\text{train}} \subseteq \mathcal{P}$, maximum reduced order $r_{\max}$, tolerance $\texttt{tol} > 0$.

Output: ROM $(\widehat{\mathcal{A}},\widehat{\mathcal{B}},\widehat{\mathcal{C}})$.

$V = [\,]$.
for i in $1, 2, \ldots, r_{\max}$ **do**
  Find $\mathsf{p}_{\max} \in \mathcal{P}_{\text{train}}$ that maximizes the error $e(\mathsf{p}) = \|y(\mathsf{p}) - \widehat{y}(\mathsf{p})\|_F$.
  if $e(\mathsf{p}_{\max}) \leq \texttt{tol}$ **then**
    Exit the **for** loop.
  Set $V = [V \quad x(\mathsf{p}_{\max})]$ and orthonormalize it.
  Form a ROM $(\widehat{\mathcal{A}},\widehat{\mathcal{B}},\widehat{\mathcal{C}})$ with $\widehat{A}_i, \widehat{B}_j, \widehat{C}_k$ as in (1.12).
Return $(\widehat{\mathcal{A}},\widehat{\mathcal{B}},\widehat{\mathcal{C}})$.

Algorithm 3.2 Proper orthogonal decomposition.

Input: FOM $(\mathcal{A},\mathcal{B},\mathcal{C})$ (1.8) in parameter-separable form (1.11), finite training set $\mathcal{P}_{\text{train}} \subseteq \mathcal{P}$, reduced order r.

Output: ROM $(\widehat{\mathcal{A}},\widehat{\mathcal{B}},\widehat{\mathcal{C}})$.

$X = [x(\mathsf{p}_1) \quad x(\mathsf{p}_2) \quad \cdots \quad x(\mathsf{p}_{|\mathcal{P}_{\text{train}}|})]$.
Compute the singular value decomposition $X = U\Sigma W^T$.
Set V as the first r columns of U.
Form a ROM $(\widehat{\mathcal{A}},\widehat{\mathcal{B}},\widehat{\mathcal{C}})$ with $\widehat{A}_i, \widehat{B}_j, \widehat{C}_k$ as in (1.12).
Return $(\widehat{\mathcal{A}},\widehat{\mathcal{B}},\widehat{\mathcal{C}})$.

3.1, where the error $\|y(\mathsf{p}) - \widehat{y}(\mathsf{p})\|_{\text{F}}$ is used instead of an error estimator. There are different error estimators proposed in the literature (see, e.g., [23, 38, 16, 12]), but our focus here is on minimizing the error and less on an efficient implementation. POD [7] is also based on a Galerkin projection and tries to find a subspace that approximates the solution set $\{x(\mathsf{p}) : \mathsf{p} \in \mathcal{P}\} \subseteq \mathbb{C}^n$ in the $\mathcal{L}_2$-optimal sense given a training set. The pseudocode for POD is given in Algorithm 3.2.

We focus on stationary parametric PDEs as numerical examples. As mentioned in Remark 2.8, the various implications of our approach for the dynamical systems case, specifically for $\mathcal{H}_2$ and $\mathcal{H}_2 \otimes \mathcal{L}_2$-optimal model order reduction of LTI systems, are presented in detail in [31]. In section 4, where we consider a discrete $\mathcal{L}_2$ norm, we include an LTI example.

In the following numerical examples, the parameter space $\mathcal{P}$ is a segment $[a, b] \subset \mathbb{R}$ and we chose $\mathcal{P}_{\text{train}} = \texttt{linspace}(a, b, 100)$ for RB and POD where `linspace` refers to the NumPy [22] method `numpy.linspace` returning a vector of equidistant points in $[a, b]$ including the boundaries. Although we describe the FOMs we use in every example, we note that $\mathcal{L}_2$-Opt-PSF only needs access to the output of the FOM and not its state or matrices. The FOM description is given since RB and POD are projection-based and work with the full-order operators.

Code availability. The source code used to compute the presented results can be obtained from [30]. The code was written in the Python programming language using pyMOR [28].

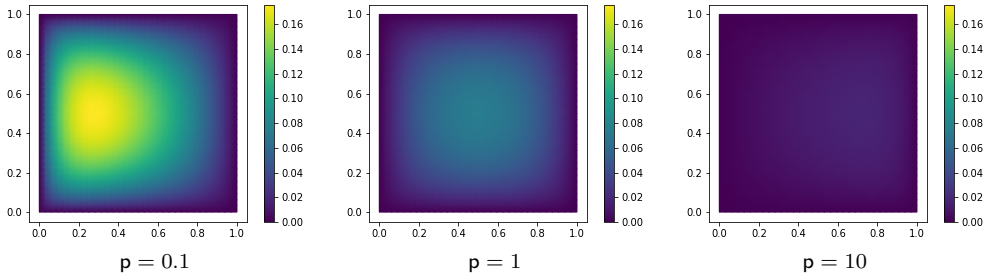

FIG. 1. *Poisson example FOM solutions for different parameter values.*

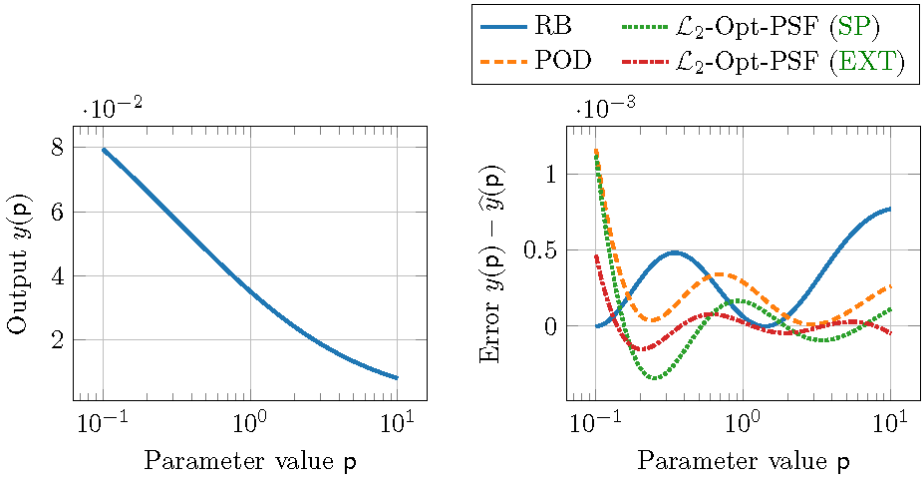

FIG. 2. *Poisson example FOM output and pointwise output errors for ROMs of order* 2.

3.1. Poisson equation. We consider the Poisson equation over the unit square $\Omega = (0,1)^2$ with homogeneous Dirichlet boundary conditions:

$$-\nabla \cdot (d(\xi,\mathsf{p})\nabla x(\xi,\mathsf{p})) = 1, \qquad \xi \in \Omega, \tag{3.1a}$$

$$x(\xi,\mathsf{p}) = 0, \qquad \xi \in \partial\Omega, \tag{3.1b}$$

where $d(\xi,\mathsf{p}) = \xi_1 + \mathsf{p}(1-\xi_1)$ and $\mathcal{P} = [0.1, 10]$. After a finite element discretization, we obtain a FOM of the form (1.4) with $n = 1089$ and $n_\mathrm{f} = 1$. For the output, we chose $C = B^\mathrm{T}$ (thus, $n_\mathrm{o} = 1$). Solutions for a few parameter values are given in Figure 1. The output can be seen in the left plot in Figure 2.

For the ROMs, we consider a structure-preserving (physics-inspired) DDROM

$$\text{(SP)} \qquad \begin{aligned} \left(\widehat{A}_1 + \mathsf{p}\widehat{A}_2\right)\widehat{x}(\mathsf{p}) &= \widehat{B}, \\ \widehat{y}(\mathsf{p}) &= \widehat{C}\widehat{x}(\mathsf{p}), \end{aligned}$$

and an extended version

$$\text{(EXT)} \qquad \begin{aligned} \left(\widehat{A}_1 + \mathsf{p}\widehat{A}_2\right)\widehat{x}(\mathsf{p}) &= \widehat{B}_1 + \mathsf{p}\widehat{B}_2, \\ \widehat{y}(\mathsf{p}) &= \left(\widehat{C}_1 + \mathsf{p}\widehat{C}_2\right)\widehat{x}(\mathsf{p}). \end{aligned}$$

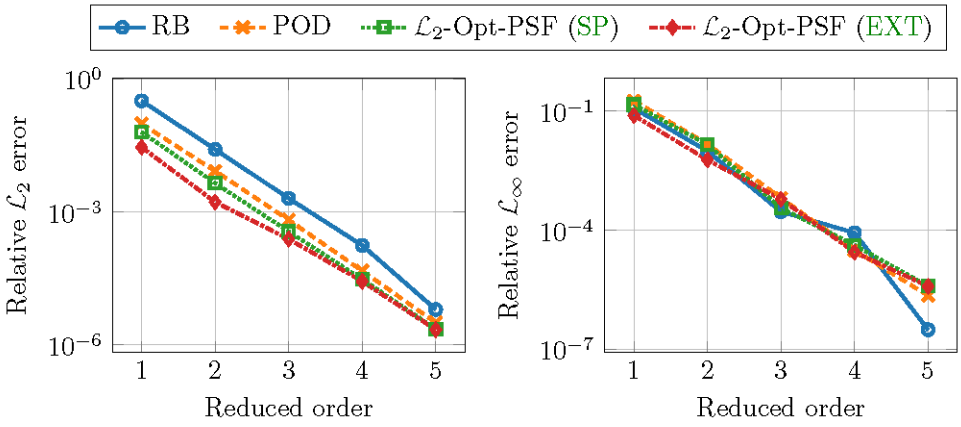

FIG. 3. *Poisson example errors for ROMs of different orders.*

We include the extended version to highlight that the proposed approach offers flexibility to include additional structures that are not necessarily present in the FOM (further emphasizing that the FOM is not needed, but only the output samples). We also note that (EXT) cannot be obtained via a state-independent linear projection.

We choose the reduced order $r = 2$. The right plot in Figure 2 shows the output errors, resulting from RB, POD, $\mathcal{L}_2$-Opt-PSF with structure preservation (initialized using POD), and $\mathcal{L}_2$-Opt-PSF with extended form (initialized using the result of structure-preserving $\mathcal{L}_2$-Opt-PSF). The relative $\mathcal{L}_2$ errors are, respectively, 2.5577×10^{-2}, 8.2483×10^{-3}, 4.3826×10^{-3}, and 1.6468×10^{-3}, illustrating that $\mathcal{L}_2$-Opt-PSF produces the smallest $\mathcal{L}_2$ error. The relative $\mathcal{L}_\infty$ errors are, respectively, 9.6919×10^{-3}, 1.4639×10^{-2}, 1.4104×10^{-2}, and 5.8541×10^{-3}. We observe that RB and POD produce ROMs with nonnegative output error. This is a general property of Galerkin projection applied to systems with symmetric positive definite $\mathcal{A}(\mathsf{p})$ and $\mathcal{B}(\mathsf{p}) = \mathcal{C}(\mathsf{p})^{\mathrm{T}}$ (see, e.g., Theorem 1.4 in [7]). We also observe that even though $\mathcal{L}_2$-Opt-PSF preserved the symmetry properties in the DDROMs, without enforcing it explicitly, it did not give DDROMs that have nonnegative output error. This implies that $\mathcal{L}_2$-Opt-PSF DDROMs are not based on Galerkin projection. An explanation for why symmetry is preserved in $\mathcal{L}_2$-Opt-PSF without explicitly enforcing it is that the gradients of the objective function (Theorem 2.7) have the same symmetry properties.

The relative $\mathcal{L}_2$ and $\mathcal{L}_\infty$ errors are shown in Figure 3 for a range of reduced orders. We observe that $\mathcal{L}_2$-Opt-PSF (SP) and $\mathcal{L}_2$-Opt-PSF (EXT) have consistently lower $\mathcal{L}_2$ error compared to POD and RB. Moreover, $\mathcal{L}_2$-Opt-PSF (SP) and $\mathcal{L}_2$-Opt-PSF (EXT) have comparable $\mathcal{L}_\infty$ errors to (and for some r values even smaller than) RB and POD even though not optimized for this error measure.

3.2. Nonseparable example. We modify the Poisson equation in (3.1) by using a diffusion term that is not parameter-separable. Specifically, we take

$$d(\xi, \mathsf{p}) = 1 - \frac{9}{10} e^{-5\left((\xi_1 - \mathsf{p})^2 + (\xi_2 - \mathsf{p})^2\right)}$$

and set $\mathcal{P} = [0, 1]$. After a finite element discretization, the FOM is of the form

$$\begin{aligned} \mathcal{A}(\mathsf{p})x(\mathsf{p}) &= B, \\ y(\mathsf{p}) &= Cx(\mathsf{p}), \end{aligned}$$

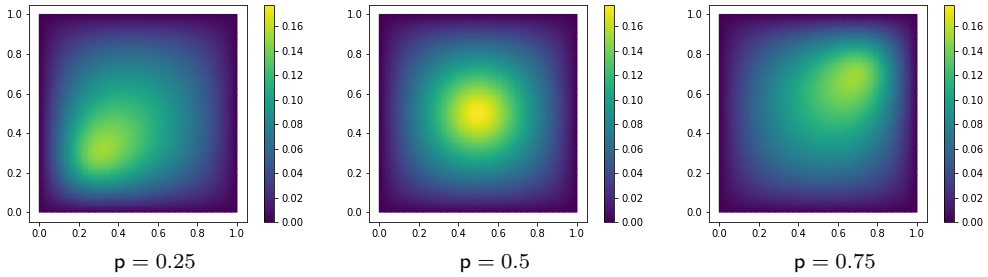

FIG. 4. *Poisson example FOM solutions for different parameter values.*

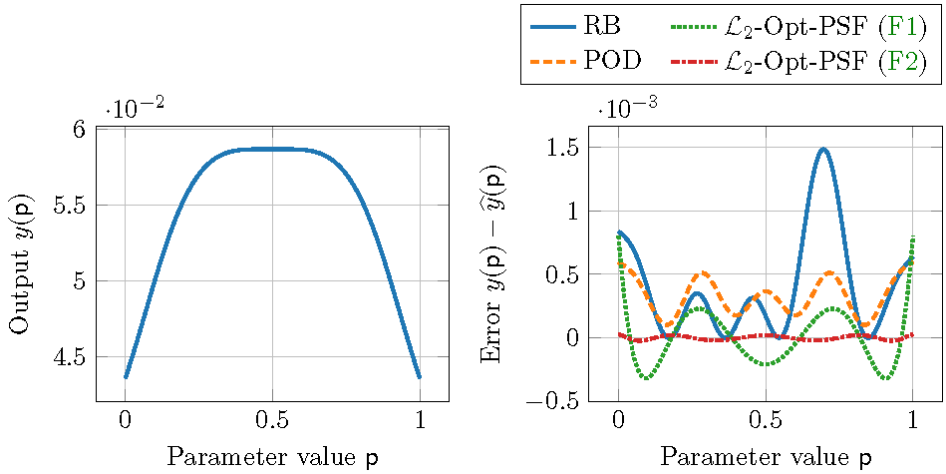

FIG. 5. *Nonseparable example FOM output and pointwise output errors for ROMs of order* 2.

with $n = 1089$ and $n_{\mathrm{f}} = 1$, and $\mathcal{A}(\mathsf{p})$ needs to be assembled for every new parameter value p. For the output, we again chose $C = B^{\mathrm{T}}$ ($n_{\mathrm{o}} = 1$). Solutions for a few parameter values are given in Figure 4. The output can be seen in the left plot in Figure 5.

Using RB or POD produces ROMs of the form

$$\begin{aligned} V^{\mathrm{T}}\mathcal{A}(\mathsf{p})V\widehat{x}(\mathsf{p}) &= V^{\mathrm{T}}B, \\ \widehat{y}(\mathsf{p}) &= CV\widehat{x}(\mathsf{p}). \end{aligned}$$

Notably, an efficient computation of $V^{\mathrm{T}}\mathcal{A}(\mathsf{p})V$ requires a further approximation of $\mathcal{A}(\mathsf{p})$ in a parameter-separable form, e.g., using the empirical interpolation method [4] as mentioned in subsection 1.1; for details, see, e.g., [9]. However, in order not to degrade the accuracy of RB and POD models, we skip that step. For the $\mathcal{L}_2$-optimal DDROMs, we consider two forms,

(F1)
$$\begin{aligned} \left(\widehat{A}_1 + \left(\mathsf{p} - \tfrac{1}{2}\right)^2 \widehat{A}_2 + \left(\mathsf{p} - \tfrac{1}{2}\right)^4 \widehat{A}_3\right)\widehat{x}(\mathsf{p}) &= \widehat{B}, \\ \widehat{y}(\mathsf{p}) &= \widehat{C}\widehat{x}(\mathsf{p}), \end{aligned}$$

TABLE 1
Relative errors for the nonseparable example.

Error measure	RB	POD	$\mathcal{L}_2$-Opt-PSF 1	$\mathcal{L}_2$-Opt-PSF 2
$\mathcal{L}_2$	1.0441×10^{-2}	6.4925×10^{-3}	3.8323×10^{-3}	2.7439×10^{-4}
$\mathcal{L}_\infty$	1.4279×10^{-2}	1.0146×10^{-2}	1.3707×10^{-2}	4.4095×10^{-4}

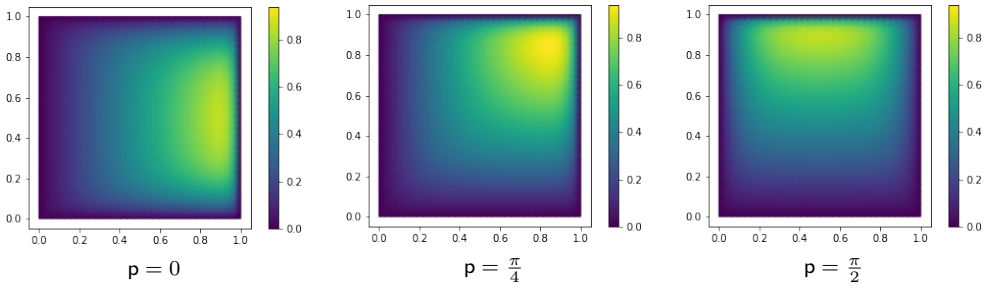

FIG. 6. *Convection-diffusion example FOM solutions for different parameter values.*

and

$$\begin{aligned}
&\left(\widehat{A}_1 + \left(\mathsf{p} - \tfrac{1}{2}\right)^2 \widehat{A}_2 + \left(\mathsf{p} - \tfrac{1}{2}\right)^4 \widehat{A}_3 + \left(\mathsf{p} - \tfrac{1}{2}\right)^6 \widehat{A}_4\right) \widehat{x}(\mathsf{p}) \\
&\qquad = \widehat{B}_1 + \left(\mathsf{p} - \tfrac{1}{2}\right)^2 \widehat{B}_2 + \left(\mathsf{p} - \tfrac{1}{2}\right)^4 \widehat{B}_3 + \left(\mathsf{p} - \tfrac{1}{2}\right)^6 \widehat{B}_4, \\
&\widehat{y}(\mathsf{p}) = \left(\widehat{C}_1 + \left(\mathsf{p} - \tfrac{1}{2}\right)^2 \widehat{C}_2 + \left(\mathsf{p} - \tfrac{1}{2}\right)^4 \widehat{C}_3 + \left(\mathsf{p} - \tfrac{1}{2}\right)^6 \widehat{C}_4\right) \widehat{x}(\mathsf{p}),
\end{aligned} \tag{F2}$$

which exploit the symmetry in $y(\mathsf{p})$ around $\mathsf{p} = \frac{1}{2}$. The right plot in Figure 5 shows the output errors of ROMs of order 4, resulting from RB, POD, and both $\mathcal{L}_2$-Opt-PSF models (both initialized with $\widehat{A}_1 = I$, $\widehat{B}_1 = \mathbf{1}$, $\widehat{C}_1 = \mathbf{1}^{\mathrm{T}}$, and $\widehat{A}_i = 0$, $\widehat{B}_i = 0$, and $\widehat{C}_i = 0$ for $i \geqslant 2$, where $\mathbf{1}$ is the vector of all ones). We observe that B and POD again produce ROMs with nonnegative output error. The relative $\mathcal{L}_2$ and $\mathcal{L}_\infty$ errors listed in Table 1 show significant improvements in $\mathcal{L}_2$ error minimization via $\mathcal{L}_2$-Opt-PSF, especially for the second DDROM form.

3.3. Convection-diffusion problem. Consider the convection-diffusion equation on the unit square $\Omega = (0,1)^2$ with homogeneous Dirichlet boundary conditions:

$$\begin{aligned}
\nabla \cdot ((\cos \mathsf{p}, \sin \mathsf{p}) x(\xi, \mathsf{p})) - \nabla \cdot (d \nabla x(\xi, \mathsf{p})) &= 1, && \xi \in \Omega, \\
x(\xi, \mathsf{p}) &= 0, && \xi \in \partial\Omega,
\end{aligned}$$

where $d = 2^{-5}$ and $\mathcal{P} = [0, 2\pi]$. For the outputs, we chose $y_\ell(\mathsf{p}) = \int_{\Omega_\ell} x(\xi, \mathsf{p}) \mathrm{d}\xi$, $\ell = 1, 2, 3, 4$, where $\Omega_1 = (0, \frac{1}{2})^2$, $\Omega_2 = (\frac{1}{2}, 1) \times (0, \frac{1}{2})$, $\Omega_3 = (\frac{1}{2}, 1)^2$, $\Omega_4 = (0, \frac{1}{2}) \times (\frac{1}{2}, 1)$. After a finite element discretization, we obtain a FOM

$$\begin{aligned}
(A_1 + \cos(\mathsf{p}) A_2 + \sin(\mathsf{p}) A_3) x(\mathsf{p}) &= B, \\
y(\mathsf{p}) &= C x(\mathsf{p}),
\end{aligned}$$

with $n = 1089$, $n_{\mathrm{f}} = 1$, and $n_{\mathrm{o}} = 4$. Solutions for a few parameter values are given in Figure 6.

The left plot in Figure 7 shows the output y.

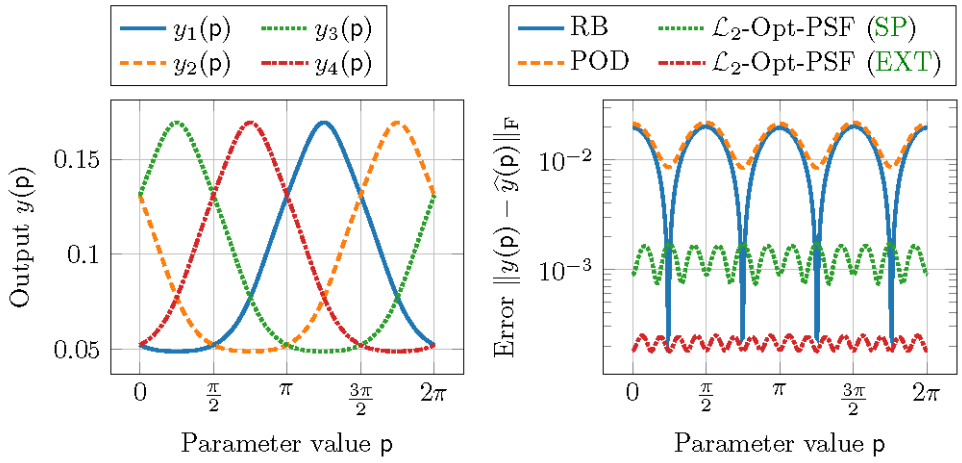

FIG. 7. *Convection-diffusion example FOM output and pointwise output error norms for ROMs of order* 4.

As for the first example, for the DDROMs, we consider a structure-preserving model

$$\text{(SP)} \qquad \begin{aligned} \left(\widehat{A}_1 + \cos(\mathsf{p})\widehat{A}_2 + \sin(\mathsf{p})\widehat{A}_3\right)\widehat{x}(\mathsf{p}) &= \widehat{B}, \\ \widehat{y}(\mathsf{p}) &= \widehat{C}\widehat{x}(\mathsf{p}), \end{aligned}$$

and an extended version

$$\text{(EXT)} \qquad \begin{aligned} \left(\widehat{A}_1 + \cos(\mathsf{p})\widehat{A}_2 + \sin(\mathsf{p})\widehat{A}_3\right)\widehat{x}(\mathsf{p}) &= \widehat{B}_1 + \cos(\mathsf{p})\widehat{B}_2 + \sin(\mathsf{p})\widehat{B}_3, \\ \widehat{y}(\mathsf{p}) &= \left(\widehat{C}_1 + \cos(\mathsf{p})\widehat{C}_2 + \sin(\mathsf{p})\widehat{C}_3\right)\widehat{x}(\mathsf{p}). \end{aligned}$$

The $\cos(\mathsf{p})$ and $\sin(\mathsf{p})$ terms are inspired by the periodicity of $y(\mathsf{p})$. The right plot in Figure 7 shows the output errors of ROMs of order 4, due to RB, POD, $\mathcal{L}_2$-Opt-PSF with structure preservation (initialized using RB), and $\mathcal{L}_2$-Opt-PSF with extended form (initialized using the structure-preserving $\mathcal{L}_2$-Opt-PSF), illustrating that both $\mathcal{L}_2$-Opt-PSF models significantly outperform RB and POD. The relative $\mathcal{L}_2$ and $\mathcal{L}_\infty$ errors for a range of reduced orders are shown in Figure 8. We observe significant improvements in both the $\mathcal{L}_2$ and $\mathcal{L}_\infty$ errors in many cases.

4. Discrete least-squares norm. So far, we have considered continuous least-squares problems where we could evaluate the parameter-to-output mapping y for any parameter value $\mathsf{p} \in \mathcal{P}$. However, in some cases, we are only given a finite set of points without a chance to reevaluate y. Furthermore, adaptive quadrature used in the previous section can be expensive for multidimensional parameter spaces. Thus, it is important to consider the *discrete* setting.

In the discrete setting where we only have samples $(\mathsf{p}_\ell, y_\ell)$, $\ell = 1, 2, \ldots, N$, we consider minimizing the mean square error (MSE)

$$\mathcal{J}_{\mathrm{MSE}} = \frac{1}{N}\sum_{\ell=1}^{N} \|y_\ell - \widehat{y}(\mathsf{p}_\ell)\|_{\mathrm{F}}^2 . \tag{4.1}$$

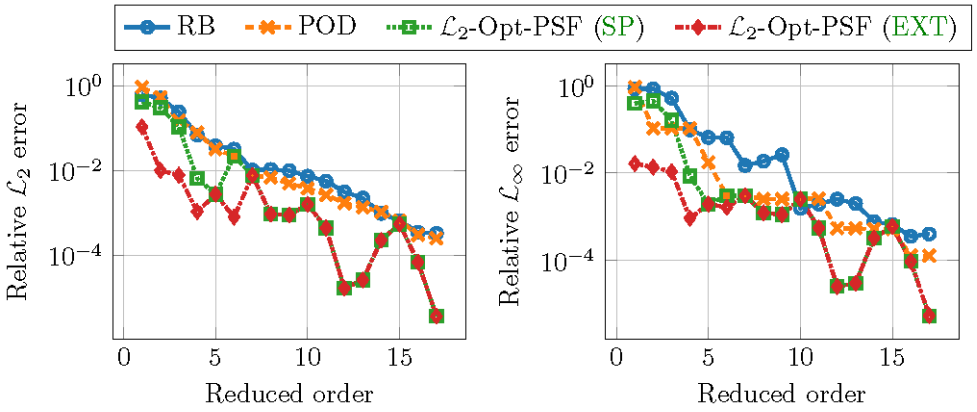

FIG. 8. *Convection-diffusion example errors for ROMs of different orders.*

Our $\mathcal{L}_2$-optimal modeling framework recovers the discrete MSE (4.1) by choosing the parameter space as $\mathcal{P} = \{\mathsf{p}_1, \mathsf{p}_2, \ldots, \mathsf{p}_N\}$ and the measure as $\mu = \frac{1}{N}\sum_{\ell=1}^{N} \delta_{\mathsf{p}_\ell}$. With these choices, the $\mathcal{L}_2$ error (1.9) becomes the MSE (4.1). Since the assumptions of Theorem 2.7 are still satisfied for the discrete measure μ, we can compute gradients, which become finite sums in this setting, as we summarize in the next result.

COROLLARY 4.1. *Let* $(\mathsf{p}_\ell, y_\ell)$, $\ell = 1, 2, \ldots, N$, *be closed under conjugation and* $(\widehat{A}_i, \widehat{B}_j, \widehat{C}_k)$ *be a tuple of DDROM matrices from* $\mathcal{R}$ (2.3). *Then, the gradients of* $\mathcal{J}_{\text{MSE}}$ (4.1) *with respect to the DDROM matrices are*

$$\nabla_{\widehat{A}_i} \mathcal{J}_{\text{MSE}} = \frac{2}{N} \sum_{\ell=1}^{N} \widehat{\alpha}_i\left(\overline{\mathsf{p}_\ell}\right) \widehat{x}_d\left(\mathsf{p}_\ell\right) \left[y_\ell - \widehat{y}\left(\mathsf{p}_\ell\right)\right] \widehat{x}\left(\mathsf{p}_\ell\right)^*, \qquad i = 1, 2, \ldots, q_{\widehat{\mathcal{A}}},$$

$$\nabla_{\widehat{B}_j} \mathcal{J}_{\text{MSE}} = \frac{2}{N} \sum_{\ell=1}^{N} \widehat{\beta}_j\left(\overline{\mathsf{p}_\ell}\right) \widehat{x}_d\left(\mathsf{p}_\ell\right) \left[\widehat{y}\left(\mathsf{p}_\ell\right) - y_\ell\right], \qquad j = 1, 2, \ldots, q_{\widehat{\mathcal{B}}},$$

$$\nabla_{\widehat{C}_k} \mathcal{J}_{\text{MSE}} = \frac{2}{N} \sum_{\ell=1}^{N} \widehat{\gamma}_k\left(\overline{\mathsf{p}_\ell}\right) \left[\widehat{y}\left(\mathsf{p}_\ell\right) - y_\ell\right] \widehat{x}\left(\mathsf{p}_\ell\right)^*, \qquad k = 1, 2, \ldots, q_{\widehat{\mathcal{C}}}.$$

Proof. The result follows directly from Theorem 2.7 by setting $\mathcal{P} = \{\mathsf{p}_1, \ldots, \mathsf{p}_N\}$, $\mu = \frac{1}{N}\sum_{\ell=1}^{N} \delta_{\mathsf{p}_\ell}$, and $y(\mathsf{p}_\ell) = y_\ell$. ∎

For the discrete setting we still use Algorithm 2.1. The only difference from the continuous setting is that we do not use adaptive quadrature, but directly evaluate the sums. As before, gradient computations only use the output samples $y(\mathsf{p}_\ell)$.

In the following we demonstrate the results on two examples; one related to LTI systems and the other arising from a Poisson equation with multiple parameters.

4.1. Flexible aircraft frequency response data. Here we use the data from [34, 37], containing samples of a transfer function $H(s)$ of an LTI dynamical system (as in (1.5)) describing the influence of wind gust on a flexible aircraft. In particular, the underlying dynamical system has $n_{\text{f}} = 1$ forcing (gust disturbance) and $n_{\text{o}} = 92$ outputs (accelerations and moments at different coordinates of a flexible aircraft wings and tail); thus in this problem $H(s) \in \mathbb{C}^{92\times 1}$. The output (transfer function) data consists of $N = 421$ pairs (ω_ℓ, H_ℓ), $\ell = 1, 2, \ldots, N$, where $\omega_\ell > 0$ are the frequencies

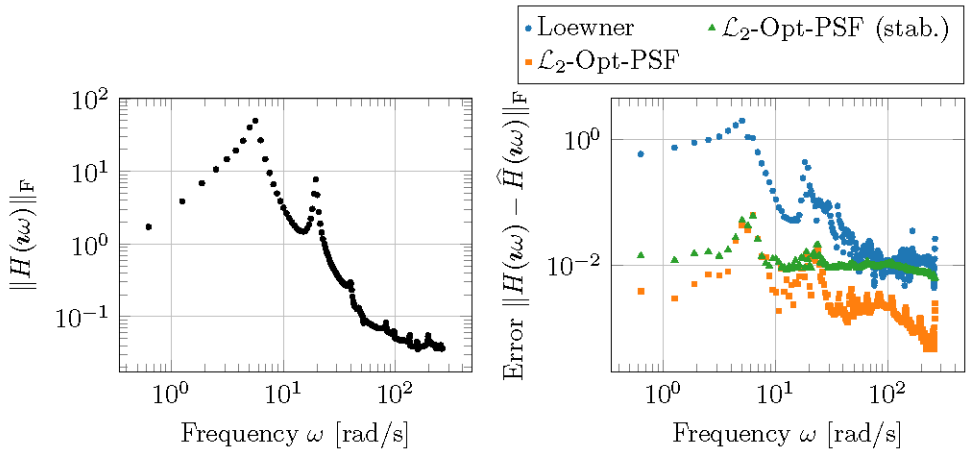

FIG. 9. *Flexible aircraft example data and pointwise output errors for ROMs of order* 100 *(*97*).*

and $H_\ell \in \mathbb{C}^{n_\mathrm{o} \times n_\mathrm{f}}$ are the frequency domain samples. The left plot in Figure 9 shows the magnitudes (norms) of the frequency responses. Our goal in this setting is to learn a DDROM of the form as in (2.4), i.e., $\widehat{H}(s) = \widehat{C}(s\widehat{E} - \widehat{A})^{-1}\widehat{B}$, that minimizes the MSE distance from the given samples $\{H_\ell\}$.

To fulfill the assumptions of Corollary 4.1, we set

$$\{(\mathsf{p}_\ell, y_\ell)\}_{\ell=1}^{2N} = \{(\imath\omega_\ell, H_\ell)\}_{\ell=1}^{N} \cup \left\{\left(-\imath\omega_\ell, \overline{H_\ell}\right)\right\}_{\ell=1}^{N}.$$

Based on this setup, we run $\mathcal{L}_2$-Opt-PSF with L-BFGS to minimize the MSE (4.1) using the optimization variables $\widehat{E}, \widehat{A} \in \mathbb{C}^{r\times r}$, $\widehat{B} \in \mathbb{C}^{r\times n_\mathrm{f}}$, and $\widehat{C} \in \mathbb{C}^{n_\mathrm{o}\times r}$. We initialize $\mathcal{L}_2$-Opt-PSF using the ROM of order $r = 100$ from [37], which uses the same data but employs the interpolatory Loewner framework [3]. We obtain a DDROM of order $r = 100$ with 3 unstable poles. Then, we project the resulting DDROM to its asymptotically stable part of order $r = 97$. Figure 9 shows the error resulting from the Loewner-based model from [37], the unstable DDROM of order 100, and its asymptotically stable part of order 97. The respective relative $\mathcal{L}_2$ errors are 4.82×10^{-2}, 1.3146×10^{-3}, and 2.5255×10^{-3}. These results illustrate that $\mathcal{L}_2$-Opt-PSF has resulted in more than one order of magnitude improvement. Moreover, the unstable part of the $\mathcal{L}_2$-Opt-PSF model was small enough that projecting it onto the asymptotically stable part did not significantly degrade the accuracy. Note that we could impose a stability constraint directly in the optimization routine, similar to [26]. Here we skipped that step to illustrate that $\mathcal{L}_2$-Opt-PSF followed by projection to the asymptotically stable part can still produce a DDROM with a small error.

Remark 4.2. In this example, the DDROM resulting from $\mathcal{L}_2$-Opt-PSF is a rational function; thus our $\mathcal{L}_2$-optimal modeling framework in this special case has solved the rational least-squares problem via a gradient-based descent algorithm. Minimizing the MSE using a rational function (rational least-square fitting) is an important problem in data-driven modeling of dynamical systems and various techniques exist; see, e.g., [39, 21, 14, 15, 25, 32, 11] and the references therein. In a future work where we specifically focus on dynamical systems and approximation of transfer functions from data, we will provide more details in this direction.

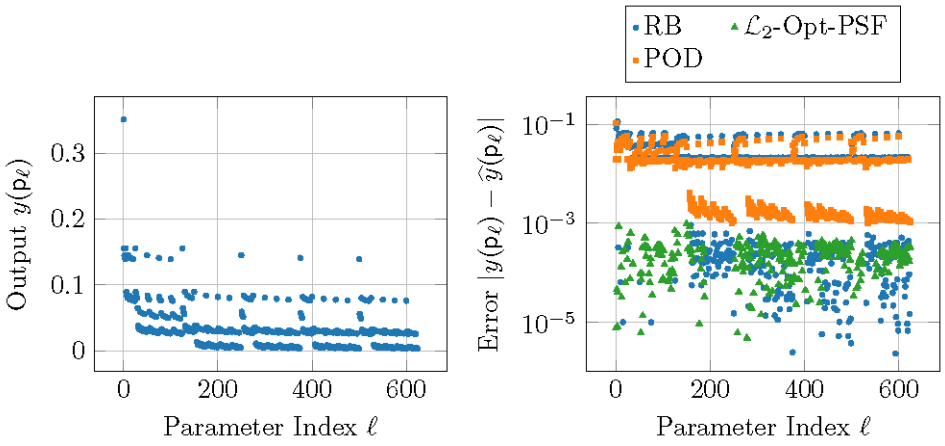

FIG. 10. *Thermal block example FOM output and pointwise output errors for ROMs of order* 4 *on the equidistant grid* $\texttt{linspace}(0.1, 10, 5)^4$ *with* $5^4 = 625$ *points.*

4.2. Thermal block example. We consider a 2×2 thermal block example over the unit square $\Omega = (0,1)^2$, i.e., we modify the Poisson equation in (3.1) by using the diffusion term

$$d(\xi, \mathsf{p}) = \mathsf{p}_1 \chi_{(0,\frac{1}{2})^2}(\xi) + \mathsf{p}_2 \chi_{(\frac{1}{2},1)\times(0,\frac{1}{2})}(\xi) + \mathsf{p}_3 \chi_{(\frac{1}{2},1)^2}(\xi) + \mathsf{p}_4 \chi_{(0,\frac{1}{2})\times(\frac{1}{2},1)}(\xi)$$

and $\mathcal{P} = [0.1, 10]^4$. Here, χ_S denotes the characteristic function of the set S, i.e., $\chi_S(\xi) = 1$ if $\xi \in S$, otherwise $\chi_S(\xi) = 0$. Therefore, the parameters $\mathsf{p}_1, \ldots, \mathsf{p}_4$ represent the diffusivity over each of the four blocks. After a finite element discretization, we obtain the FOM of the form

$$\begin{aligned}(A_0 + \mathsf{p}_1 A_1 + \mathsf{p}_2 A_2 + \mathsf{p}_3 A_3 + \mathsf{p}_4 A_4)\, x(\mathsf{p}) &= B,\\ y(\mathsf{p}) &= Cx(\mathsf{p}),\end{aligned}$$

with $n = 1089$ and $n_\mathrm{f} = 1$. For the output, we kept $C = B^\mathrm{T}$. The left plot in Figure 10 shows the output of the FOM over the equidistant grid $\mathcal{P}_\mathrm{test} = \texttt{linspace}(0.1, 10, 5)^4$.

We look for structure-preserving DDROMs of the same form:

$$\begin{aligned}\left(\widehat{A}_0 + \mathsf{p}_1 \widehat{A}_1 + \mathsf{p}_2 \widehat{A}_2 + \mathsf{p}_3 \widehat{A}_3 + \mathsf{p}_4 \widehat{A}_4\right) \widehat{x}(\mathsf{p}) &= \widehat{B},\\ \widehat{y}(\mathsf{p}) &= \widehat{C}\widehat{x}(\mathsf{p}).\end{aligned}$$

We choose $r = 4$ as the reduced order. We construct two projection-based ROMs using RB and POD trained on the grid $\mathcal{P}_\mathrm{train} = \texttt{linspace}(0.1, 10, 4)^4$. Then, using only the discrete output samples $y(\mathsf{p}_\ell)$ from the same training grid, i.e., a total of $N = 4^4 = 256$ output samples $y(\mathsf{p}_\ell)$, we run the discrete $\mathcal{L}_2$-Opt-PSF (initialized with the POD ROM) to minimize the MSE (4.1). Figure 10 shows the outputs and the resulting errors over $\mathcal{P}_\mathrm{test}$. The figure shows a significant reduction of the errors for the $\mathcal{L}_2$ DDROM. We note that $\mathcal{P}_\mathrm{test}$ and $\mathcal{P}_\mathrm{train}$ overlap only on $2^4 = 16$ points (corners) out of $5^4 = 625$ test parameter values. The relative $\mathcal{L}_2$ errors over $\mathcal{P}_\mathrm{test}$ for RB, POD, and $\mathcal{L}_2$-Opt-PSF are, respectively, 6.037×10^{-1}, 4.8002×10^{-1}, and 1.0266×10^{-2}.

5. $\mathcal{L}_2$-optimal DDROMs and projection-based ROMs. RB and POD, as implemented in section 3, use Galerkin projection. In section 3, we found that $\mathcal{L}_2$-optimal DDROMs obtained via Algorithm 2.1 are not based on Galerkin projection

for the compliant Poisson examples. The question remains whether the $\mathcal{L}_2$-optimal DDROMs can be constructed by a (state-independent) Petrov–Galerkin projection. The answer is clearly "no" when the FOM and DDROM are of different structure, in particular, when the DDROM has an additional nonzero term as we have in our extended $\mathcal{L}_2$-optimal DDROMs. Therefore, we consider the case when the two models have the same parameter-separable forms as in (2.1). Let $\widehat{\mathcal{A}}(\mathsf{p})$, $\widehat{\mathcal{B}}(\mathsf{p})$, and $\widehat{\mathcal{C}}(\mathsf{p})$ be the DDROM quantities obtained via Algorithm 2.1. We want to see if there exist $V, W \in \mathbb{R}^{n\times r}$ of full rank such that

$$\widehat{\mathcal{A}}(\mathsf{p}) = W^{\mathrm{T}}\mathcal{A}(\mathsf{p})V, \quad \widehat{\mathcal{B}}(\mathsf{p}) = W^{\mathrm{T}}\mathcal{B}(\mathsf{p}), \quad \widehat{\mathcal{C}}(\mathsf{p}) = \mathcal{C}(\mathsf{p})V.$$

Assuming that the sets of scalar functions $\{\widehat{\alpha}_i\}_{i=1}^{q_{\widehat{\mathcal{A}}}}$, $\{\widehat{\beta}_j\}_{j=1}^{q_{\widehat{\mathcal{B}}}}$, and $\{\widehat{\gamma}_k\}_{k=1}^{q_{\widehat{\mathcal{C}}}}$ are linearly independent, this is equivalent to

$$\widehat{A}_i = W^{\mathrm{T}}A_iV, \qquad i = 1, 2, \ldots, q_{\widehat{\mathcal{A}}}, \tag{5.1a}$$

$$\widehat{B}_j = W^{\mathrm{T}}B_j, \qquad j = 1, 2, \ldots, q_{\widehat{\mathcal{B}}}, \tag{5.1b}$$

$$\widehat{C}_k = C_kV, \qquad k = 1, 2, \ldots, q_{\widehat{\mathcal{C}}}. \tag{5.1c}$$

We observe that (5.1) is a system of nonlinear equations, generally difficult to analyze. However, the equations containing B_j and C_k are linear, which we exploit next.

By vertically stacking (5.1c), we obtain the linear system $\mathbf{C}V = \widehat{\mathbf{C}}$, where

$$\mathbf{C} = \begin{bmatrix} C_1^{\mathrm{T}} & \cdots & C_{q_{\widehat{\mathcal{C}}}}^{\mathrm{T}} \end{bmatrix}^{\mathrm{T}} \quad \text{and} \quad \widehat{\mathbf{C}} = \begin{bmatrix} \widehat{C}_1^{\mathrm{T}} & \cdots & \widehat{C}_{q_{\widehat{\mathcal{C}}}}^{\mathrm{T}} \end{bmatrix}^{\mathrm{T}}. \tag{5.2}$$

If $\mathbf{C}$ is of full row rank (in particular, $q_{\widehat{\mathcal{C}}} n_{\mathrm{o}} \leqslant n$), using its singular value decomposition

$$\mathbf{C} = U_{\mathbf{C}} \begin{bmatrix} \Sigma_{\mathbf{C}} & 0 \end{bmatrix} \begin{bmatrix} V_{\mathbf{C},1} & V_{\mathbf{C},2} \end{bmatrix}^{\mathrm{T}}, \tag{5.3}$$

we can write the solution to $\mathbf{C}V = \widehat{\mathbf{C}}$ as

$$V = \underbrace{V_{\mathbf{C},1}\Sigma_{\mathbf{C}}^{-1}{U_{\mathbf{C}}}^{\mathrm{T}}\widehat{\mathbf{C}}}_{=:V_1} + V_{\mathbf{C},2}X \tag{5.4}$$

for some $X \in \mathbb{R}^{(n-q_{\widehat{\mathcal{C}}}n_{\mathrm{o}})\times r}$. Similarly, we find that

$$W = \underbrace{U_{\mathbf{B},1}\Sigma_{\mathbf{B}}^{-1}{V_{\mathbf{B}}}^{\mathrm{T}}\widehat{\mathbf{B}}^{\mathrm{T}}}_{=:W_1} + U_{\mathbf{B},2}Y \tag{5.5}$$

for some $Y \in \mathbb{R}^{(n-q_{\widehat{\mathcal{B}}}n_{\mathrm{f}})\times r}$, where

$$\mathbf{B} = \begin{bmatrix} B_1 & \cdots & B_{q_{\widehat{\mathcal{B}}}} \end{bmatrix}, \quad \widehat{\mathbf{B}} = \begin{bmatrix} \widehat{B}_1 & \cdots & \widehat{B}_{q_{\widehat{\mathcal{B}}}} \end{bmatrix}, \tag{5.6}$$

$$\mathbf{B} = \begin{bmatrix} U_{\mathbf{B},1} \\ U_{\mathbf{B},2} \end{bmatrix}^{\mathrm{T}} \begin{bmatrix} \Sigma_{\mathbf{B}} \\ 0 \end{bmatrix} V_{\mathbf{B}}^{\mathrm{T}}, \tag{5.7}$$

assuming that $\mathbf{B}$ is of full column rank. Then, from (5.1a), we obtain

$$(W_1 + U_{\mathbf{B},2}Y)^{\mathrm{T}}A_iV_{\mathbf{C},2}X = \widehat{A}_i - (W_1 + U_{\mathbf{B},2}Y)^{\mathrm{T}}A_iV_1, \quad i = 1, 2, \ldots, q_{\widehat{\mathcal{A}}}. \tag{5.8}$$

Stacking all the quantities, we obtain

$$\begin{bmatrix} (W_1 + U_{\mathbf{B},2}Y)^{\mathrm{T}}A_1V_{\mathbf{C},2} \\ \vdots \\ (W_1 + U_{\mathbf{B},2}Y)^{\mathrm{T}}A_{q_{\widehat{\mathcal{A}}}}V_{\mathbf{C},2} \end{bmatrix} X = \begin{bmatrix} \widehat{A}_1 - (W_1 + U_{\mathbf{B},2}Y)^{\mathrm{T}}A_1V_1 \\ \vdots \\ \widehat{A}_{q_{\widehat{\mathcal{A}}}} - (W_1 + U_{\mathbf{B},2}Y)^{\mathrm{T}}A_{q_{\widehat{\mathcal{A}}}}V_1 \end{bmatrix},$$

which is a system of $r^2 q_{\widehat{\mathcal{A}}}$ equations and $r(n - q_{\widehat{\mathcal{C}}}n_{\mathrm{o}})$ unknowns. Assuming that the system matrix is of full row rank, there is at least one X that solves the system. Thus we have just proved the following result.

THEOREM 5.1. *Let* $\mathbf{B}$ *in* (5.6) *be of full column rank and* $\mathbf{C}$ *in* (5.2) *of full row rank. Let their singular value decompositions be given by* (5.7) *and* (5.3). *Also, let* V_1 *and* W_2 *be as in* (5.4) *and* (5.5). *If there exists* $Y \in \mathbb{R}^{(n-q_{\widehat{\mathcal{B}}}n_{\mathrm{f}})\times r}$ *such that*

$$\begin{bmatrix} (W_1 + U_{\mathbf{B},2}Y)^{\mathrm{T}} A_1 V_{\mathbf{C},2} \\ \vdots \\ (W_1 + U_{\mathbf{B},2}Y)^{\mathrm{T}} A_{q_{\widehat{\mathcal{A}}}} V_{\mathbf{C},2} \end{bmatrix} \in \mathbb{R}^{q_{\widehat{\mathcal{A}}}r\times(n-q_{\widehat{\mathcal{C}}}n_{\mathrm{o}})}$$

is of full row rank, then there exist $V, W \in \mathbb{R}^{n\times r}$ *satisfying* (5.1).

This result says that, in the generic case, all DDROMs with the same parameter-separable form as the FOM can be formed using Petrov–Galerkin projection, including $\mathcal{L}_2$-optimal ones. Note that a similar, dual result to Theorem 5.1 can be obtained by fixing X and solving for Y in (5.8).

6. Conclusions. We presented a gradient-based descent algorithm to construct data-driven $\mathcal{L}_2$-optimal reduced-order models that only requires access to output samples. By appropriately defining the measure and parameter space, the framework we developed covers both continuous (Lebesgue) and discrete cost functions, and stationary and dynamical systems. The various numerical examples illustrated the efficiency of the proposed $\mathcal{L}_2$-optimal modeling approach. Moreover, we have developed the generic conditions for a DDROM to be projection-based. The gradients derived in this paper have direct implications for and connections to interpolatory model reduction methods and these issues will be revisited in a separate work.

Appendix A. Proof of Lemma 2.6. First, we show that $\mathcal{R}$ is an open subset of R. Let $(\widehat{A}_i, \widehat{B}_j, \widehat{C}_k) \in \mathcal{R}$ be arbitrary. The definition of $\mathcal{R}$ (2.3) yields

$$|\widehat{\alpha}_i(\mathsf{p})| \left\|\widehat{\mathcal{A}}(\mathsf{p})^{-1}\right\|_{\mathrm{F}} \leqslant M \text{ for all } i = 1, 2, \ldots, q_{\widehat{\mathcal{A}}} \text{ and for } \mu\text{-almost all } \mathsf{p} \in \mathcal{P} \tag{A.1}$$

for some $M > 0$. Then let $\Delta\widehat{A}_i \in \mathbb{R}^{r\times r}$ for $i = 1, 2, \ldots, q_{\widehat{\mathcal{A}}}$, with $\sum_{\bar{\imath}=1}^{q_{\widehat{\mathcal{A}}}} \|\Delta\widehat{A}_{\bar{\imath}}\|_{\mathrm{F}} \leqslant \frac{1}{2M}$, be arbitrary. For μ-almost all $\mathsf{p} \in \mathcal{P}$, using (A.1) in the second inequality, we obtain

$$\left\|\sum_{\bar{\imath}=1}^{q_{\widehat{\mathcal{A}}}} \widehat{\alpha}_{\bar{\imath}}(\mathsf{p})\Delta\widehat{A}_{\bar{\imath}}\widehat{\mathcal{A}}(\mathsf{p})^{-1}\right\|_{\mathrm{F}} \leqslant \sum_{\bar{\imath}=1}^{q_{\widehat{\mathcal{A}}}} |\widehat{\alpha}_{\bar{\imath}}(\mathsf{p})| \left\|\widehat{\mathcal{A}}(\mathsf{p})^{-1}\right\|_{\mathrm{F}} \left\|\Delta\widehat{A}_{\bar{\imath}}\right\|_{\mathrm{F}} \leqslant M \sum_{\bar{\imath}=1}^{q_{\widehat{\mathcal{A}}}} \left\|\Delta\widehat{A}_{\bar{\imath}}\right\|_{\mathrm{F}} \leqslant \frac{1}{2}. \tag{A.2}$$

In the following, our goal is to show that $(\widehat{A}_i + \Delta\widehat{A}_i, \widehat{B}_j, \widehat{C}_k) \in \mathcal{R}$. To start, we have

$$\begin{aligned} |\widehat{\alpha}_i(\mathsf{p})| \left\|\left(\sum_{\bar{\imath}=1}^{q_{\widehat{\mathcal{A}}}} \widehat{\alpha}_{\bar{\imath}}(\mathsf{p}) \left(\widehat{A}_{\bar{\imath}} + \Delta\widehat{A}_{\bar{\imath}}\right)\right)^{-1}\right\|_{\mathrm{F}} &= |\widehat{\alpha}_i(\mathsf{p})| \left\|\left(\widehat{\mathcal{A}}(\mathsf{p}) + \sum_{\bar{\imath}=1}^{q_{\widehat{\mathcal{A}}}} \widehat{\alpha}_{\bar{\imath}}(\mathsf{p})\Delta\widehat{A}_{\bar{\imath}}\right)^{-1}\right\|_{\mathrm{F}} \\ &= |\widehat{\alpha}_i(\mathsf{p})| \left\|\widehat{\mathcal{A}}(\mathsf{p})^{-1}\left(I + \sum_{\bar{\imath}=1}^{q_{\widehat{\mathcal{A}}}} \widehat{\alpha}_{\bar{\imath}}(\mathsf{p})\Delta\widehat{A}_{\bar{\imath}}\widehat{\mathcal{A}}(\mathsf{p})^{-1}\right)^{-1}\right\|_{\mathrm{F}} \\ &\leqslant |\widehat{\alpha}_i(\mathsf{p})| \left\|\widehat{\mathcal{A}}(\mathsf{p})^{-1}\right\| \left\|\left(I + \sum_{\bar{\imath}=1}^{q_{\widehat{\mathcal{A}}}} \widehat{\alpha}_{\bar{\imath}}(\mathsf{p})\Delta\widehat{A}_{\bar{\imath}}\widehat{\mathcal{A}}(\mathsf{p})^{-1}\right)^{-1}\right\|_{\mathrm{F}}. \end{aligned}$$

Using that $\|(I-X)^{-1}\|_{\mathrm{F}} \leqslant \frac{1}{1-\|X\|_{\mathrm{F}}}$ for all $X \in \mathbb{C}^{r\times r}$ such that $\|X\|_{\mathrm{F}} < 1$, from (A.2) and (A.1) we get

$$|\widehat{\alpha}_i(\mathsf{p})| \left\| \left(\sum_{\bar{\imath}=1}^{q_{\widehat{\mathcal{A}}}} \widehat{\alpha}_{\bar{\imath}}(\mathsf{p}) \left(\widehat{A}_{\bar{\imath}} + \Delta\widehat{A}_{\bar{\imath}} \right) \right)^{-1} \right\|_{\mathrm{F}} \leqslant |\widehat{\alpha}_i(\mathsf{p})| \left\| \widehat{\mathcal{A}}(\mathsf{p})^{-1} \right\|_{\mathrm{F}} \frac{1}{1-\frac{1}{2}} \leqslant 2M < \infty$$

for μ-almost every $\mathsf{p} \in \mathcal{P}$. Therefore, we have $(\widehat{A}_i + \Delta\widehat{A}_i, \widehat{B}_j, \widehat{C}_k) \in \mathcal{R}$. Since $\widehat{B}_j$ and $\widehat{C}_k$ are arbitrary, it follows that there is an open neighborhood of $(\widehat{A}_i, \widehat{B}_j, \widehat{\mathcal{C}}_k)$ in $\mathcal{R}$.

Next we prove that $\|\widehat{y}\|_{\mathcal{L}_2(\mathcal{P},\mu)} < \infty$. Note that from (A.1), if $\widehat{\alpha}_i(\mathsf{p}) \neq 0$, then $\|\widehat{\mathcal{A}}(\mathsf{p})^{-1}\|_{\mathrm{F}} \leqslant \frac{M}{|\widehat{\alpha}_i(\mathsf{p})|}$. Furthermore, note that the set of parameter values $\mathsf{p} \in \mathcal{P}$ such that $\widehat{\alpha}_i(\mathsf{p}) = 0$ for all $i = 1, 2, \ldots, q_{\widehat{\mathcal{A}}}$ forms a set of μ-measure zero (otherwise, this would contradict (2.2)). Therefore,

$$\left\| \widehat{\mathcal{A}}(\mathsf{p})^{-1} \right\|_{\mathrm{F}} \leqslant \min_i \frac{M}{|\widehat{\alpha}_i(\mathsf{p})|} \leqslant \frac{M}{\max_i |\widehat{\alpha}_i(\mathsf{p})|} \text{ for } \mu\text{-almost all } \mathsf{p} \in \mathcal{P}. \tag{A.3}$$

Using submultiplicativity and the triangle inequality, we obtain

$$\begin{aligned} \|\widehat{y}\|_{\mathcal{L}_2}^2 &= \int_{\mathcal{P}} \left\| \widehat{\mathcal{C}}(\mathsf{p}) \widehat{\mathcal{A}}(\mathsf{p})^{-1} \widehat{\mathcal{B}}(\mathsf{p}) \right\|_{\mathrm{F}}^2 \mathrm{d}\mu(\mathsf{p}) \\ &\leqslant \int_{\mathcal{P}} \left\| \widehat{\mathcal{C}}(\mathsf{p}) \right\|_{\mathrm{F}}^2 \left\| \widehat{\mathcal{A}}(\mathsf{p})^{-1} \right\|_{\mathrm{F}}^2 \left\| \widehat{\mathcal{B}}(\mathsf{p}) \right\|_{\mathrm{F}}^2 \mathrm{d}\mu(\mathsf{p}) \\ &\leqslant \int_{\mathcal{P}} \left(\sum_{k=1}^{q_{\widehat{\mathcal{C}}}} |\widehat{\gamma}_k(\mathsf{p})| \left\| \widehat{C}_k \right\|_{\mathrm{F}} \right)^2 \left\| \widehat{\mathcal{A}}(\mathsf{p})^{-1} \right\|_{\mathrm{F}}^2 \left(\sum_{j=1}^{q_{\widehat{\mathcal{B}}}} \left| \widehat{\beta}_j(\mathsf{p}) \right| \left\| \widehat{B}_j \right\|_{\mathrm{F}} \right)^2 \mathrm{d}\mu(\mathsf{p}). \end{aligned} \tag{A.4}$$

Using $\|\widehat{B}_j\|_{\mathrm{F}} \leqslant \max_{\bar{\jmath}} \|\widehat{B}_{\bar{\jmath}}\|_{\mathrm{F}}$ and $\|\widehat{C}_k\|_{\mathrm{F}} \leqslant \max_{\bar{k}} \|\widehat{C}_{\bar{k}}\|_{\mathrm{F}}$, we find

$$\|\widehat{y}\|_{\mathcal{L}_2}^2 \leqslant \max_{\bar{\jmath}} \left\| \widehat{B}_{\bar{\jmath}} \right\|_{\mathrm{F}}^2 \max_{\bar{k}} \left\| \widehat{C}_{\bar{k}} \right\|_{\mathrm{F}}^2 \int_{\mathcal{P}} \left(\sum_{j=1}^{q_{\widehat{\mathcal{B}}}} \left| \widehat{\beta}_j(\mathsf{p}) \right| \right)^2 \left(\sum_{k=1}^{q_{\widehat{\mathcal{C}}}} |\widehat{\gamma}_k(\mathsf{p})| \right)^2 \left\| \widehat{\mathcal{A}}(\mathsf{p})^{-1} \right\|_{\mathrm{F}}^2 \mathrm{d}\mu(\mathsf{p}).$$

Next, using (A.3), we obtain

$$\|\widehat{y}\|_{\mathcal{L}_2}^2 \leqslant M^2 \max_{\bar{\jmath}} \left\| \widehat{B}_{\bar{\jmath}} \right\|_{\mathrm{F}}^2 \max_{\bar{k}} \left\| \widehat{C}_{\bar{k}} \right\|_{\mathrm{F}}^2 \int_{\mathcal{P}} \frac{\left(\sum_{j=1}^{q_{\widehat{\mathcal{B}}}} \left| \widehat{\beta}_j(\mathsf{p}) \right| \right)^2 \left(\sum_{k=1}^{q_{\widehat{\mathcal{C}}}} |\widehat{\gamma}_k(\mathsf{p})| \right)^2}{\max_i |\widehat{\alpha}_i(\mathsf{p})|^2} \mathrm{d}\mu(\mathsf{p}).$$

Finally, using that $\max_{i=1,2,\ldots,n} x_i \geqslant \sqrt{(\sum_{i=1}^n x_i^2)/n}$ for nonnegative numbers x_i,

$$\|\widehat{y}\|_{\mathcal{L}_2}^2 \leqslant {q_{\widehat{\mathcal{A}}}}^2 M^2 \max_{\bar{\jmath},\bar{k}} \left\| \widehat{B}_{\bar{\jmath}} \right\|_{\mathrm{F}}^2 \left\| \widehat{C}_{\bar{k}} \right\|_{\mathrm{F}}^2 \int_{\mathcal{P}} \frac{\left(\sum_{j=1}^{q_{\widehat{\mathcal{B}}}} \left| \widehat{\beta}_j(\mathsf{p}) \right| \right)^2 \left(\sum_{k=1}^{q_{\widehat{\mathcal{C}}}} |\widehat{\gamma}_k(\mathsf{p})| \right)^2}{\left(\sum_{i=1}^{q_{\widehat{\mathcal{A}}}} |\widehat{\alpha}_i(\mathsf{p})| \right)^2} \mathrm{d}\mu(\mathsf{p}) < \infty,$$

which completes the proof.

Appendix B. Proof of Theorem 2.7. Rewrite the objective function as

$$\mathcal{J} = \|y\|_{\mathcal{L}_2(\mathcal{P},\mu)}^2 \tag{B.1a}$$

$$- 2 \int_{\mathcal{P}} \operatorname{tr}\left(y(\mathsf{p})^* \widehat{\mathcal{C}}(\mathsf{p}) \widehat{\mathcal{A}}(\mathsf{p})^{-1} \widehat{\mathcal{B}}(\mathsf{p}) \right) \mathrm{d}\mu(\mathsf{p}) \tag{B.1b}$$

$$+ \int_{\mathcal{P}} \operatorname{tr}\left(\widehat{\mathcal{B}}(\mathsf{p})^* \widehat{\mathcal{A}}(\mathsf{p})^{-*} \widehat{\mathcal{C}}(\mathsf{p})^* \widehat{\mathcal{C}}(\mathsf{p}) \widehat{\mathcal{A}}(\mathsf{p})^{-1} \widehat{\mathcal{B}}(\mathsf{p}) \right) \mathrm{d}\mu(\mathsf{p}), \tag{B.1c}$$

where we used the fact that $\langle y, \widehat{y}\rangle_{\mathcal{L}_2(\mathcal{P},\mu)} = \langle \widehat{y}, y\rangle_{\mathcal{L}_2(\mathcal{P},\mu)} \in \mathbb{R}$ (Assumption 2.1). The part of $\mathcal{J}$ in (B.1a) does not depend on the reduced quantities, so it does not contribute to the gradient. Let $\mathcal{J}_2$ denote the second term (B.1b) in the cost function $\mathcal{J}$, i.e.,

$$\mathcal{J}_2 = -2\int_{\mathcal{P}} \operatorname{tr}\left(y(\mathsf{p})^*\widehat{\mathcal{C}}(\mathsf{p})\widehat{\mathcal{A}}(\mathsf{p})^{-1}\widehat{\mathcal{B}}(\mathsf{p})\right)\mathrm{d}\mu(\mathsf{p}).$$

We start by computing $\nabla_{\widehat{A}_i}\mathcal{J}_2$. To do so, we evaluate $\mathcal{J}_2(\widehat{A}_i + \Delta\widehat{A}_i)$ for a perturbation $\Delta\widehat{A}_i$ to obtain

$$\begin{aligned}\mathcal{J}_2\left(\widehat{A}_i + \Delta\widehat{A}_i\right) &= -2\int_{\mathcal{P}} \operatorname{tr}\left(y(\mathsf{p})^*\widehat{\mathcal{C}}(\mathsf{p})\left(\widehat{\mathcal{A}}(\mathsf{p}) + \widehat{\alpha}_i(\mathsf{p})\Delta\widehat{A}_i\right)^{-1}\widehat{\mathcal{B}}(\mathsf{p})\right)\mathrm{d}\mu(\mathsf{p})\\ &= -2\int_{\mathcal{P}} \operatorname{tr}\left(y(\mathsf{p})^*\widehat{\mathcal{C}}(\mathsf{p})\left(I + \widehat{\alpha}_i(\mathsf{p})\widehat{\mathcal{A}}(\mathsf{p})^{-1}\Delta\widehat{A}_i\right)^{-1}\widehat{\mathcal{A}}(\mathsf{p})^{-1}\widehat{\mathcal{B}}(\mathsf{p})\right)\mathrm{d}\mu(\mathsf{p}).\end{aligned}$$

Assuming small enough $\Delta\widehat{A}_i$, using the property in (2.3), and applying the Neumann series formula yield

$$\begin{aligned}\mathcal{J}_2\left(\widehat{A}_i + \Delta\widehat{A}_i\right) &= -2\int_{\mathcal{P}} \operatorname{tr}\left(y(\mathsf{p})^*\widehat{\mathcal{C}}(\mathsf{p})\widehat{\mathcal{A}}(\mathsf{p})^{-1}\widehat{\mathcal{B}}(\mathsf{p})\right)\mathrm{d}\mu(\mathsf{p})\\ &\quad + 2\int_{\mathcal{P}} \operatorname{tr}\left(\widehat{\alpha}_i(\mathsf{p})y(\mathsf{p})^*\widehat{\mathcal{C}}(\mathsf{p})\widehat{\mathcal{A}}(\mathsf{p})^{-1}\Delta\widehat{A}_i\widehat{\mathcal{A}}(\mathsf{p})^{-1}\widehat{\mathcal{B}}(\mathsf{p})\right)\mathrm{d}\mu(\mathsf{p})\\ &\quad - 2\int_{\mathcal{P}} \operatorname{tr}\left(y(\mathsf{p})^*\widehat{\mathcal{C}}(\mathsf{p})\sum_{m=2}^{\infty}\left(-\widehat{\alpha}_i(\mathsf{p})\widehat{\mathcal{A}}(\mathsf{p})^{-1}\Delta\widehat{A}_i\right)^m\widehat{\mathcal{A}}(\mathsf{p})^{-1}\widehat{\mathcal{B}}(\mathsf{p})\right)\mathrm{d}\mu(\mathsf{p})\\ &= \mathcal{J}(\widehat{A}_i) + \left\langle 2\int_{\mathcal{P}}\overline{\widehat{\alpha}_i(\mathsf{p})}\widehat{\mathcal{A}}(\mathsf{p})^{-*}\widehat{\mathcal{C}}(\mathsf{p})^*y(\mathsf{p})\widehat{\mathcal{B}}(\mathsf{p})^*\widehat{\mathcal{A}}(\mathsf{p})^{-*}\mathrm{d}\mu(\mathsf{p}), \Delta\widehat{A}_i\right\rangle_{\mathrm{F}}\\ &\quad - 2\sum_{m=2}^{\infty}\int_{\mathcal{P}} \operatorname{tr}\left(y(\mathsf{p})^*\widehat{\mathcal{C}}(\mathsf{p})\left(-\widehat{\alpha}_i(\mathsf{p})\widehat{\mathcal{A}}(\mathsf{p})^{-1}\Delta\widehat{A}_i\right)^m\widehat{\mathcal{A}}(\mathsf{p})^{-1}\widehat{\mathcal{B}}(\mathsf{p})\right)\mathrm{d}\mu(\mathsf{p}).\end{aligned} \tag{B.2}$$

First, we check that the candidate for the gradient, resulting from the second term in the last equation, is indeed bounded:

$$\begin{aligned}&\left\|\int_{\mathcal{P}}\widehat{\alpha}_i(\overline{\mathsf{p}})\widehat{\mathcal{A}}(\mathsf{p})^{-*}\widehat{\mathcal{C}}(\mathsf{p})^*y(\mathsf{p})\widehat{\mathcal{B}}(\mathsf{p})^*\widehat{\mathcal{A}}(\mathsf{p})^{-*}\mathrm{d}\mu(\mathsf{p})\right\|_{\mathrm{F}}\\ &\quad\leqslant \int_{\mathcal{P}}|\widehat{\alpha}_i(\mathsf{p})|\left\|\widehat{\mathcal{A}}(\mathsf{p})^{-1}\right\|_{\mathrm{F}}\left\|\widehat{\mathcal{C}}(\mathsf{p})\right\|_{\mathrm{F}}\left\|\widehat{\mathcal{A}}(\mathsf{p})^{-1}\right\|_{\mathrm{F}}\left\|\widehat{\mathcal{B}}(\mathsf{p})\right\|_{\mathrm{F}}\|y(\mathsf{p})\|_{\mathrm{F}}\,\mathrm{d}\mu(\mathsf{p})\\ &\quad\leqslant \left\|\widehat{\alpha}_i(\cdot)\widehat{\mathcal{A}}(\cdot)^{-1}\right\|_{\mathcal{L}_\infty(\mathcal{P},\mu)}\int_{\mathcal{P}}\left\|\widehat{\mathcal{C}}(\mathsf{p})\right\|_{\mathrm{F}}\left\|\widehat{\mathcal{A}}(\mathsf{p})^{-1}\right\|_{\mathrm{F}}\left\|\widehat{\mathcal{B}}(\mathsf{p})\right\|_{\mathrm{F}}\|y(\mathsf{p})\|_{\mathrm{F}}\,\mathrm{d}\mu(\mathsf{p}) < \infty,\end{aligned}$$

where we used (2.2) and (2.3) (see (A.4) in the proof of Lemma 2.6). Second, we check that the remaining terms in (B.2) are of lower order:

$$\begin{aligned}&\left|\sum_{m=2}^{\infty}\int_{\mathcal{P}} \operatorname{tr}\left(y(\mathsf{p})^*\widehat{\mathcal{C}}(\mathsf{p})\left(-\widehat{\alpha}_i(\mathsf{p})\widehat{\mathcal{A}}(\mathsf{p})^{-1}\Delta\widehat{A}_i\right)^m\widehat{\mathcal{A}}(\mathsf{p})^{-1}\widehat{\mathcal{B}}(\mathsf{p})\right)\mathrm{d}\mu(\mathsf{p})\right|\\ &\leqslant_{\mathcal{L}_2(\mathcal{P},\mu)} y\|_{\mathcal{L}_2(\mathcal{P},\mu)}\sum_{m=2}^{\infty}\left\|\widehat{\mathcal{C}}(\cdot)\left(-\widehat{\alpha}_i(\cdot)\widehat{\mathcal{A}}(\cdot)^{-1}\Delta\widehat{A}_i\right)^m\widehat{\mathcal{A}}(\cdot)^{-1}\widehat{\mathcal{B}}(\cdot)\right\|_{\mathcal{L}_2(\mathcal{P},\mu)}\\ &\leqslant \|y\|_{\mathcal{L}_2(\mathcal{P},\mu)}\sum_{m=2}^{\infty}\left\|\widehat{\alpha}_i(\cdot)\widehat{\mathcal{A}}(\cdot)^{-1}\right\|_{\mathcal{L}_\infty}^m\left\|\|\widehat{\mathcal{C}}(\cdot)\|_{\mathrm{F}}\|\widehat{\mathcal{A}}(\cdot)^{-1}\|_{\mathrm{F}}\|\widehat{\mathcal{B}}(\cdot)\|_{\mathrm{F}}\right\|_{\mathcal{L}_2(\mathcal{P},\mu)}\|\Delta\widehat{A}_i\|_{\mathrm{F}}^m\end{aligned}$$

$$= \|y\|_{\mathcal{L}_2(\mathcal{P},\mu)} \left\| \|\widehat{\mathcal{C}}(\cdot)\|_{\mathrm{F}} \|\widehat{\mathcal{A}}(\cdot)^{-1}\|_{\mathrm{F}} \|\widehat{\mathcal{B}}(\cdot)\|_{\mathrm{F}} \right\|_{\mathcal{L}_2(\mathcal{P},\mu)} \frac{\left\|\widehat{\alpha}_i(\cdot)\widehat{\mathcal{A}}(\cdot)^{-1}\right\|_{\mathcal{L}_\infty}^2 \|\Delta\widehat{A}_i\|_{\mathrm{F}}^2}{1 - \left\|\widehat{\alpha}_i(\cdot)\widehat{\mathcal{A}}(\cdot)^{-1}\right\|_{\mathcal{L}_\infty} \|\Delta\widehat{A}_i\|_{\mathrm{F}}}$$

$$= o\left(\|\Delta\widehat{A}_i\|_{\mathrm{F}}\right).$$

Therefore,

$$\nabla_{\widehat{A}_i}\mathcal{J}_2 = 2\int_{\mathcal{P}} \widehat{\alpha}_i(\overline{\mathsf{p}})\widehat{\mathcal{A}}(\mathsf{p})^{-*}\widehat{\mathcal{C}}(\mathsf{p})^* y(\mathsf{p})\widehat{\mathcal{B}}(\mathsf{p})^*\widehat{\mathcal{A}}(\mathsf{p})^{-*}\mathrm{d}\mu(\mathsf{p}).$$

Next, we compute $\nabla_{\widehat{B}_j}\mathcal{J}_2$ similarly by evaluating $\mathcal{J}_2(\widehat{B}_j + \Delta\widehat{B}_j)$:

$$\begin{aligned}
\mathcal{J}_2\left(\widehat{B}_j + \Delta\widehat{B}_j\right) &= -2\int_{\mathcal{P}} \mathrm{tr}\left(y(\mathsf{p})^*\widehat{\mathcal{C}}(\mathsf{p})\widehat{\mathcal{A}}(\mathsf{p})^{-1}\left(\widehat{\mathcal{B}}(\mathsf{p}) + \widehat{\beta}_j(\mathsf{p})\Delta\widehat{B}_j\right)\right)\mathrm{d}\mu(\mathsf{p}) \\
&= \mathcal{J}_2(\widehat{B}_j) - 2\int_{\mathcal{P}} \mathrm{tr}\left(\widehat{\beta}_j(\mathsf{p})y(\mathsf{p})^*\widehat{\mathcal{C}}(\mathsf{p})\widehat{\mathcal{A}}(\mathsf{p})^{-1}\Delta\widehat{B}_j\right)\mathrm{d}\mu(\mathsf{p}) \\
&= \mathcal{J}_2(\widehat{B}_j) - 2\left\langle \int_{\mathcal{P}} \widehat{\beta}_j(\overline{\mathsf{p}})\widehat{\mathcal{A}}(\mathsf{p})^{-*}\widehat{\mathcal{C}}(\mathsf{p})^* y(\mathsf{p})\mathrm{d}\mu(\mathsf{p}), \Delta\widehat{B}_j \right\rangle_{\mathrm{F}}.
\end{aligned}$$

It follows from (2.2) and (2.3) that the mapping $\mathsf{p} \mapsto \widehat{\beta}_j(\overline{\mathsf{p}})\widehat{\mathcal{A}}(\mathsf{p})^{-*}\widehat{\mathcal{C}}(\mathsf{p})^*$ is square-integrable. Therefore

$$\nabla_{\widehat{B}_j}\mathcal{J}_2 = -2\int_{\mathcal{P}} \widehat{\beta}_j(\overline{\mathsf{p}})\widehat{\mathcal{A}}(\mathsf{p})^{-*}\widehat{\mathcal{C}}(\mathsf{p})^* y(\mathsf{p})\mathrm{d}\mu(\mathsf{p}).$$

Similarly, one can obtain

$$\nabla_{\widehat{C}_k}\mathcal{J}_2 = -2\int_{\mathcal{P}} \widehat{\gamma}_k(\overline{\mathsf{p}}) y(\mathsf{p})\widehat{\mathcal{B}}(\mathsf{p})^*\widehat{\mathcal{A}}(\mathsf{p})^{-*}\mathrm{d}\mu(\mathsf{p}).$$

Finally, after differentiating the last part of $\mathcal{J}$ in (B.1c), we obtain

$$\begin{aligned}
\nabla_{\widehat{A}_i}\mathcal{J} &= 2\int_{\mathcal{P}} \widehat{\alpha}_i(\overline{\mathsf{p}})\widehat{\mathcal{A}}(\mathsf{p})^{-*}\widehat{\mathcal{C}}(\mathsf{p})^*\left(y(\mathsf{p}) - \widehat{\mathcal{C}}(\mathsf{p})\widehat{\mathcal{A}}(\mathsf{p})^{-1}\widehat{\mathcal{B}}(\mathsf{p})\right)\widehat{\mathcal{B}}(\mathsf{p})^*\widehat{\mathcal{A}}(\mathsf{p})^{-*}\mathrm{d}\mu(\mathsf{p}), \\
\nabla_{\widehat{B}_j}\mathcal{J} &= 2\int_{\mathcal{P}} \widehat{\beta}_j(\overline{\mathsf{p}})\widehat{\mathcal{A}}(\mathsf{p})^{-*}\widehat{\mathcal{C}}(\mathsf{p})^*\left(\widehat{\mathcal{C}}(\mathsf{p})\widehat{\mathcal{A}}(\mathsf{p})^{-1}\widehat{\mathcal{B}}(\mathsf{p}) - y(\mathsf{p})\right)\mathrm{d}\mu(\mathsf{p}), \quad \text{and} \\
\nabla_{\widehat{C}_k}\mathcal{J} &= 2\int_{\mathcal{P}} \widehat{\gamma}_k(\overline{\mathsf{p}})\left(\widehat{\mathcal{C}}(\mathsf{p})\widehat{\mathcal{A}}(\mathsf{p})^{-1}\widehat{\mathcal{B}}(\mathsf{p}) - y(\mathsf{p})\right)\widehat{\mathcal{B}}(\mathsf{p})^*\widehat{\mathcal{A}}(\mathsf{p})^{-*}\mathrm{d}\mu(\mathsf{p}),
\end{aligned}$$

which completes the proof.

REFERENCES

[1] A. C. Antoulas, *Approximation of Large-Scale Dynamical Systems,* Adv. Des. Control 6, SIAM, Philadelphia, 2005.

[2] A. C. Antoulas, C. A. Beattie, and S. Gugercin, *Interpolatory model reduction of large-scale dynamical systems*, in Efficient Modeling and Control of Large-Scale Systems, J. Mohammadpour and K. M. Grigoriadis, eds., Springer US, Boston, MA, 2010, pp. 3–58, https://doi.org/10.1007/978-1-4419-5757-3˙1.

[3] A. C. Antoulas, C. A. Beattie, and S. Gugercin, *Interpolatory Methods for Model Reduction*, Comput. Sci. Eng. 21, SIAM, Philadelphia, 2020.

[4] M. Barrault, Y. Maday, N. C. Nguyen, and A. T. Patera, *An empirical interpolation method: Application to efficient reduced-basis discretization of partial differential equations*, C. R. Math., 339 (2004), pp. 667–672, https://doi.org/10.1016/j.crma.2004.08.006.

[5] U. Baur, C. A. Beattie, P. Benner, and S. Gugercin, *Interpolatory projection methods for parameterized model reduction*, SIAM J. Sci. Comput., 33 (2011), pp. 2489–2518, https://doi.org/10.1137/090776925.

[6] P. Benner, P. Goyal, and I. P. Duff, *Identification of Dominant Subspaces for Linear Structured Parametric Systems and Model Reduction*, https://arxiv.doi.org/10.48550/1910.13945, math.NA, 2019.

[7] P. Benner, S. Grivet-Talocia, A. Quarteroni, G. Rozza, W. Schilders, and L. M. Silveira, eds., Model Order Reduction: Volume 2*: Snapshot-Based Methods and Algorithms*, De Gruyter, Berlin, 2020, https://doi.org/10.1515/9783110671490.

[8] P. Benner, S. Grivet-Talocia, A. Quarteroni, G. Rozza, W. Schilders, and L. M. Silveira, eds., *Model Order Reduction: Volume* 1*: System- and Data-Driven Methods and Algorithms*, De Gruyter, Berlin, 2021, https://doi.org/10.1515/9783110498967.

[9] P. Benner, S. Gugercin, and K. Willcox, *A survey of projection-based model reduction methods for parametric dynamical systems*, SIAM Rev., 57 (2015), pp. 483–531, https://doi.org/10.1137/130932715.

[10] P. Benner, M. Ohlberger, A. Cohen, and K. Willcox, *Model Reduction and Approximation*, SIAM, Philadelphia, 2017, https://doi.org/10.1137/1.9781611974829,

[11] M. Berljafa and S. Güttel, *The RKFIT algorithm for nonlinear rational approximation*, SIAM J. Sci. Comput., 39 (2017), pp. A2049–A2071, https://doi.org/10.1137/15M1025426.

[12] Y. Chen, J. Jiang, and A. Narayan, *A robust error estimator and a residual-free error indicator for reduced basis methods*, Comput. Math. Appl., 77 (2019), pp. 1963–1979, https://doi.org/10.1016/j.camwa.2018.11.032.

[13] P. G. Constantine, E. Dow, and Q. Wang, *Active subspace methods in theory and practice: Applications to kriging surfaces*, SIAM J. Sci. Comput., 36 (2014), pp. A1500–A1524, https://doi.org/10.1137/130916138.

[14] Z. Drmač, S. Gugercin, and C. Beattie, *Quadrature-based vector fitting for discretized $\mathcal{H}_2$ approximation*, SIAM J. Sci. Comput., 37 (2015), pp. A625–A652, https://doi.org/10.1137/140961511.

[15] Z. Drmač, S. Gugercin, and C. Beattie, *Vector fitting for matrix-valued rational approximation*, SIAM J. Sci. Comput., 37 (2015), pp. A2346–A2379, https://doi.org/10.1137/15M1010774.

[16] L. Feng and P. Benner, *A new error estimator for reduced-order modeling of linear parametric systems*, IEEE Trans. Microw. Theory Techn., 67 (2019), pp. 4848–4859, https://doi.org/10.1109/TMTT.2019.2948858.

[17] A. R. Grimm, *Parametric Dynamical Systems: Transient Analysis and Data Driven Modeling*, Ph.D. thesis, Virginia Polytechnic Institute and State University, 2018, http://hdl.handle.net/10919/83840.

[18] S. Gugercin, A. C. Antoulas, and C. Beattie, *$\mathcal{H}_2$ model reduction for large-scale linear dynamical systems*, SIAM J. Matrix Anal. Appl., 30 (2008), pp. 609–638, https://doi.org/10.1137/060666123.

[19] S. Gugercin, A. C. Antoulas, and C. A. Beattie. *A rational Krylov iteration for optimal $\mathcal{H}_2$ model reduction*, in Proceedings of the 17th International Symposium on Mathematical Theory of Networks and Systems, 2006, pp. 1665–1667.

[20] S. Gugercin, T. Stykel, and S. Wyatt, *Model reduction of descriptor systems by interpolatory projection methods*, SIAM J. Sci. Comput., 35 (2013), pp. B1010–B1033, https://doi.org/10.1137/130906635.

[21] B. Gustavsen and A. Semlyen, *Rational approximation of frequency domain responses by vector fitting*, IEEE Trans. Power Del., 14 (1999), pp. 1052–1061, https://doi.org/10.1109/61.772353.

[22] C. R. Harris, K. J. Millman, S. J. van der Walt, et al., *Array programming with NumPy*, Nature, 585 (2020), pp. 357–362, https://doi.org/10.1038/s41586-020-2649-2.

[23] J. S. Hesthaven, G. Rozza, and B. Stamm, *Certified Reduced Basis Methods for Parametrized Partial Differential Equations*, Springer Briefs Math., Springer, Cham, Switzerland, 2016.

[24] C. Himpe and M. Ohlberger, *Cross-Gramian-based combined state and parameter reduction for large-scale control systems*, Math. Probl. Eng., 2014 (2014), pp. 1–13, https://doi.org/10.1155/2014/843869.

[25] J. M. Hokanson and C. C. Magruder, *$\mathcal{H}_2$-optimal model reduction using projected nonlinear least squares*, SIAM J. Sci. Comput., 42 (2020), pp. A4017–A4045, https://doi.org/10.1137/19M1247863.

[26] M. Hund, T. Mitchell, P. Mlinarić, and J. Saak, *Optimization-based parametric model order reduction via $\mathcal{H}_2 \otimes \mathcal{L}_2$ first-order necessary conditions*, SIAM J. Sci. Comput., 44 (2022), pp. A1554–A1578, https://doi.org/10.1137/21M140290X.

[27] V. Mehrmann and T. Stykel, *Balanced truncation model reduction for large-scale systems in descriptor form*, in Dimension Reduction of Large-Scale Systems, P. Benner, V. Mehrmann, and D. C. Sorensen, eds., Lect. Notes Comput. Sci. Eng. 45, Springer-Verlag, Berlin, 2005, pp. 83–115, https://doi.org/10.1007/3-540-27909-1_3.

[28] R. Milk, S. Rave, and F. Schindler, *pyMOR—generic algorithms and interfaces for model order reduction*, SIAM J. Sci. Comput., 38 (2016), pp. S194–S216, https://doi.org/10.1137/15M1026614.

[29] T. Mitchell, *Solving problems in reduced order modeling via nonsmooth constrained optimization and fast approximation*, in Workshop on Model Reduction Methods and Optimization, 2016, https://www.mathos.unios.hr/index.php/443.

[30] P. Mlinarić, *$\mathcal{L}_2$-Optimal Reduced-Order Modeling Eexperiments*, 2022, https://github.com/pmli/l2-opt-rom-ex/tree/v1.

[31] P. Mlinarić and S. Gugercin, *A Unifying Framework for Interpolatory $\mathcal{L}_2$-Optimal Reduced-Order Modeling*, 2022, https://doi.org/10.48550/arXiv.2209.00714.

[32] Y. Nakatsukasa, O. Sète, and L. N. Trefethen, *The AAA algorithm for rational approximation*, SIAM J. Sci. Comput., 40 (2018), pp. A1494–A1522, https://doi.org/10.1137/16M1106122.

[33] J. Nocedal and S. J. Wright, *Numerical Optimization*, Springer, New York, 1999, https://doi.org/10.1007/b98874.

[34] *Flexible Aircraft*, Model Order Reduction Wiki, 2021, http://modelreduction.org/index.php/Flexible_Aircraft.

[35] B. Peherstorfer and K. Willcox, *Data-driven operator inference for nonintrusive projection-based model reduction*, Comput. Methods Appl. Mech. Engrg., 306 (2016), pp. 196–215, https://doi.org/10.1016/j.cma.2016.03.025.

[36] D. Petersson, *A Nonlinear Optimization Approach to $\mathcal{H}_2$-Optimal Modeling and Control,* dissertation, Linköping University, 2013, http://liu.diva-portal.org/smash/get/diva2:647068/FULLTEXT01.pdf.

[37] C. Poussot-Vassal, D. Quero, and P. Vuillemin, *Data-driven approximation of a high fidelity gust-oriented flexible aircraft dynamical model*, in IFAC PapersOnLine, 51 (2018), pp. 559–564, https://doi.org/10.1016/j.ifacol.2018.03.094.

[38] A. Quarteroni, A. Manzoni, and F. Negri, *Reduced Basis Methods for Partial Differential Equations: An Introduction*, UNITEXT, Springer, Cham, Switzerland, 2016.

[39] C. Sanathanan and J. Koerner, *Transfer function synthesis as a ratio of two complex polynomials*, IEEE Trans. Automat. Control, 8 (1963), pp. 56–58, https://doi.org/10.1109/TAC.1963.1105517.

[40] P. Schwerdtner and M. Voigt, *SOBMOR: Structured Optimization-Based Model Order Reduction*, https://arxiv.doi.org/10.48550/2011.07567, 2020.

[41] P. Virtanen, R. Gommers, T. E. Oliphant, et al., *SciPy* 1.0*: Fundamental algorithms for scientific computing in Python*, Nat. Methods, 17 (2020), pp. 261–272, https://doi.org/10.1038/s41592-019-0686-2.